Single-cell transcriptomics-based multidisease analysis revealing the molecular dynamics of retinal neurovascular units under inflammatory and hypoxic conditions

Yuxi Zhang
The Second Clinical School of Southern Medical University
Xiongyi Yang
The Second Clinical School of Southern Medical University
Xiaoqing Deng
The Second Clinical School of Southern Medical University
Siyu Yang
The Seventh Affiliated Hospital of Sun Yat-Sen University
Qiumo Li
The Second Clinical School of Southern Medical University
Zhuohang Xie
The Second Clinical School of Southern Medical University
Libing Hong
The Second Clinical School of Southern Medical University
Mingzhe Cao
The Seventh Affiliated Hospital of Sun Yat-Sen University
Guoguo Yi
The Sixth Affiliated Hospital Sun Yat-Sen University
Min Fu (min_fu1212@163.com)
Zhujiang Hospital, Southern Medical University

Research Article

Keywords: Retinal Neurovascular Unit, Single-Cell RNA Sequencing, Bioinformatics, Müller cells, Experimental Autoimmune Uveitis, Familial Exudative Vitreoretinopathy

Posted Date: July 29th, 2022

DOI: https://doi.org/10.21203/rs.3.rs-1888726/v1

Abstract

The retinal neurovascular unit (NVU) is paramount to maintaining the homeostasis of the retina and determines the progression of various diseases, including diabetic retinopathy (DR), glaucoma, and retinopathy of prematurity (ROP). Although some studies have investigated these diseases, a combined analysis of disease-wide etiology in the NUV at the single-cell level is lacking. Herein, we constructed an atlas of the NVU under inflammatory and hypoxic conditions by integrating single-cell transcriptome data from retinas from wild-type, AireKO, and NdpKO mice. Based on the heterogeneity of the NVU structure and transcriptome diversity under normal and pathological conditions, we discovered two subpopulations of Müller cells: Aqp4^{hi} and Aqp4^{lo} cells. Specifically, Aqp4^{lo} cells expresses phototransduction genes and represent a special type of Müller cell distinct from Aqp4^{hi} cells, classical Müller cells. AireKO mice exhibit experimental autoimmune uveitis (EAU) with severe damage to the NVU structure, mainly degeneration of Aqp4^{hi} cells. NdpKO mice exhibited familial exudative vitreoretinopathy (FEVR), with damage to the endothelial barrier, endothelial cell tight junction destruction and basement membrane thickening, accompanied by the reactive secretion of proangiogenic factors by Aqp4^{hi} cells. In both EAU and FEVR, Aqp4^{hi} cells are a key factor leading to NVU damage, and the mechanism by which they are generated is regulated by different transcription factors. By studying the pattern of immune cell infiltration in AireKO mice, we constructed a regulatory loop of "inflammatory cells/NVU - monocytes - APCs - *Ifng*$^{+}$ T cells", providing a new target for blocking the inflammatory cascade. Our elucidation of the cell-specific molecular changes, cell–cell interactions and transcriptional mechanisms of the retinal NVU provides new insights to support the development of multipurpose drugs to block or even reverse NVU damage.

1 Introduction

The neurovascular unit (NVU) is a group of closely associated neuronal cells, microvessels, and glial cells that essentially function as a single unit in the nervous system(1). Recently, the NVU in the retina has attracted increasing interest due to its irreplaceable role in maintaining neuronal survival and retinal homeostasis(2). Once exposed to pathological conditions such as inflammation or hypoxia, the NVU is structurally destroyed, and this accelerates disease progression as an independent pathogenic factor. To amplify, in retinal vascular diseases such as diabetic retinopathy (DR), retinal vascular occlusion (RVO) and retinopathy of prematurity (ROP), NVU damage triggers inflammation and oxidative stress, resulting in neuronal apoptosis(3, 4). Therefore, in-depth research on the NVU in the retina is vital and will not only provide new insight for exploring the etiology of retinal diseases but also contribute to the development of precise or personalized medicines.

Despite significant progress in understanding the NVU in terms of the etiology of retinal diseases, previous studies have focused on only a single disease. For example, in DR, the NVU was found to exhibit dysregulation of intercellular signaling and communication pathways between cells, which triggers retinal leakage and neuronal degeneration and threatens vision in the early stages(5). In glaucoma, the alterations in the NVU include oxidative stress related to impaired neurovascular coupling in the retina,

which exacerbates axonal degeneration(6). However, to the best of our knowledge, a disease-wide study of the NVU to overcome case-specific differences is still lacking.

In this regard, a combined bioinformatics analysis of the NVU in the context of multiple pathological changes provides a feasible and cost-effective approach to fill this gap. An appealing method is based on the easily available yet powerful single-cell RNA sequencing (ScRNA-seq) technique(7), which allows deep sequencing and the identification of associations at the cellular level, supporting elucidation of the complexity of the NVU as well as the heterogeneity between cells in terms of cellular subtypes and internal communications. Such a combined analysis can help to construct a transcriptional atlas of the cells in the NVU, reveal transcriptome diversity between normal and pathological states, map gene expression associated with different diseases to specific cellular compartments, and identify common pathological features of the NVU among different diseases; all of these outcomes contribute to the development of multipurpose drugs.

This study represents the first attempt to analyze the NVU in three different states, the normal state and two typical disease models, inflammation and hypoxia. Specifically, these two pathological states were chosen to cover all representative diseases of the retina due to their generalizability. The data used for the combined analysis were all obtained from the public data (GSE132229, GSE125708; mouse datasets) uploaded by Jeremy Nathans' team on the Gene Expression Omnibus website (GEO)(8, 9). Specifically, Aire knockout (AireKO) mice were used as a representative model of inflammation, clinically manifested as experimental autoimmune uveitis (EAU); Ndp knockout (NdpKO) mice were used as a representative model of hypoxia, clinically manifested as familial exudative vitreoretinopathy (FEVR); and wild-type (WT) mice were used as normal samples.

We mapped the single-cell transcriptome of the NVU under physiological and pathological conditions to characterize the cellular and molecular features of EAU and FEVR. We reveal the heterogeneity of the NVU, characterize two resident Müller cell subtypes and elucidate their biological properties and transcriptional regulatory mechanisms. Our study comprehensively characterizes the infiltration of immune cells in the NVU, revealing the profile of the inflammatory cascade. In conclusion, our study elucidates the important role of the NVU in retinal diseases, provides a comprehensive analysis of the NVU in two different states (AireKO and NdpKO), and provides insights for the development of new therapies to alleviate disease progression.

2 Results

2.1 A single-cell atlas of the mouse retina in the normal state and two pathological states

2.1.1 Retinal microstructure: Tertiary neuronal structure and the neurovascular unit

The retina is a highly specialized neural tissue that encodes and transmits visual information to the visual center (10). Its structure includes the following. 1) Tertiary neuron structure: Photoreceptors (rods and cones) convert photons into electrochemical signals and transmit signals to secondary neurons through neurotransmitters; interneurons (bipolar cells (BCs), horizontal cells (HCs), and amacrine cells (ACs)) process and transmit visual signals; and output neurons (retinal ganglion cells (RGCs)) conduct signals through axons to the visual cortex (11, 12). 2) The microvascular system (endothelial cells, pericytes and the outer basement membrane) forms and maintains the blood–retinal barrier (BRB) and transports nutrients and oxygen to meet the high metabolic demand of the retina (13). 3) Macroglia (astrocytes and Müller cells) encapsulate retinal neurons and blood vessels, participate in the formation of the BRB and maintain the homeostasis of the retinal environment (13). 4) Microglia and a small number of perivascular macrophages (PVMs) act as resident immune cells to monitor changes in the retinal microenvironment (14) (Figure 1A). The retinal neurovascular unit (NVU) is composed of glial cells, vasculature, and neurons (3, 5). Since astrocytes are mainly confined to the inner retina and wrap the blood vessels and neuronal axons in the ganglion cell layer (13), the NVU of the ganglion cell layer is mainly discussed below. The cellular components include astrocytes, Müller cells, endothelial cells, pericytes, and RGCs.

2.1.2 Source of data and cell regrouping

To explore the pathological changes in the NVU in different diseases at single-cell resolution, we collected retinal data from Aire knockout (AireKO) and Ndp knockout (NdpKO) mice. Data for the analysis were derived from publicly available data uploaded by Jeremy Nathans' team (8, 9). AIRE (AutoImmune Regulator) regulates the expression of tissue-specific antigens, including retinoid binding protein (IRBP) and retinal soluble antigen (S-Ag) (15). AireKO mice develop multiorgan autoimmune disease characterized by experimental autoimmune uveitis (EAU) in the eye. NdpKO mice exhibit abnormal retinal peripheral blood vessel formation due to disturbances in the Norrin/β-catenin signaling pathway, resulting in retinal hypoxia (16, 17). NdpKO mice serve as a good model for familial exudative vitreoretinopathy (FEVR). A total of 94,622 single-cell transcripts were obtained from a comprehensive analysis of transcriptomic data from these two studies, including 4 AireKO samples, 2 NdpKO samples, and 6 wild-type (WT) samples. Based on strict quality control, 61,953 cells ultimately passed the filtration steps, of which 21,469 were from AireKO mice, 10,218 were from NdpKO mice, and 30,266 were from WT mice (Figure S1A). After unbiased clustering of the data, 53 clusters were obtained (Figure S1B-D). Based on the original article and canonical cell markers(8, 9, 18, 19), we identified resident retinal cells and infiltrating immune cells in AireKO mice (including 1) T lymphocytes, B lymphocytes, and plasma cells; 2) the monocyte lineage; and 3) NK cells) (Figure 1B). Meanwhile, some subclusters containing rods, cones and Müller cells were only present in AireKO mice (Figure 1C). This is attributed to changes in the cellular phenotype caused by the inflammatory environment, in which neuronal degeneration in uveitis has also been demonstrated in other studies(20). We also identified some strongly and specifically expressed genes in intrinsic retinal cell types (Figure 1D), providing new insights for the identification and characterization of retinal cells.

2.1.3 Sample for verification: "P14"

The retinas of seven 14-day-old WT mice obtained by Aviv Regev and Steven A. McCarroll were used to verify our conclusion and were named sample "P14" (21). The screening conditions and processing workflow were completely consistent with those used for the data in the analysis. P14 was divided into 58 subclusters, and the corresponding cell types were identified according to the original article. All clusters in P14 were used to validate the newly obtained cell markers, and a perfect fit was achieved (Figure 1E and S2A-C).

2.1.4 Differentially expressed genes of AireKO and NdpKO mice compared with WT mice

We calculated the number of differentially expressed genes (DEGs) in retinal intrinsic cell types in AireKO and NdpKO mice compared with WT mice. Differences in Müller cells were most pronounced in AireKO mice, whereas differences in endothelial cells and Müller cells were most prominent in NdpKO mice (Figure 1F). Meanwhile, in both models, the NVU was more prone to changes than the neurons of the phototransduction system.

We also show the specific up- and downregulated genes for each cell type (Figure 1G). Consistent with the original article, almost all retinal cells in AireKO mice showed upregulation of MHC-II genes, which are involved in antigen presentation and promote immune cell infiltration, thereby aggravating the inflammatory response. Notably, astrocytes, Müller cells, and endothelial cells showed downregulation of genes that maintain their own function, suggesting that all three cell types were severely damaged in AireKO mice. In NdpKO mice, Müller cells and endothelial cells showed upregulation of *Vegfa* and *Igfbp3*, which are involved in promoting neovascularization in response to hypoxia. The majority of cells in the NdpKO mice showed downregulation of genes in the Xist family, which were confirmed to inhibit hypoxia-induced cell death in cardiomyocytes(22). We speculate that the downregulation of Xist family genes is a self-protection mechanism of retinal cells.

2.1.5 Alterations in cellular communication in AireKO and NdpKO cells

CellChat was used to calculate communication signals in normal retinas to analyze cellular crosstalk(23). The cellular communication among Müller cells, astrocytes and RGCs is particularly active, and the complex signal exchange among the three cell types is conducive to maintaining the survival of RGCs (Figure 1H). We also calculated changes in the number of signals released and received by retinal cells in both models (Figure 1I). In AireKO mice, macrophages and macroglia significantly upregulated communication signals (predominantly inflammatory signals), while tertiary neurons downregulated communication signals, suggesting impairment of phototransduction. Communication signaling in

Müller cells, astrocytes, and endothelial cells was upregulated in NdpKO mice, while that in tertiary neurons was almost unchanged, suggesting that the BRB was initially affected.

2.2 Exploration and validation of two subpopulations of Müller cells

Müller cells not only scavenges synaptic glutamate but also expel excess water through aquaporin 4 (*Aqp4*) on terminal foot processes facing the vitreous or capillary endothelium, preventing intraretinal fluid accumulation(24). Impaired Aqp4 results in decreased permeability of the plasma membrane and edema of the cell body in Müller cells; these changes are considered early pathophysiological events in diseases such as neuromyelitis optica spectrum disorders (NMOSDs)(25) and diabetic macular edema (DME)(26).

2.2.1 Two Müller cell subpopulations

Due to the integration of multiple samples, a large number of Müller cell transcripts were obtained and separated into two subpopulations with significant differences (Figure 2A, S2D and S3A). Both subpopulations expressed typical markers of Müller cells. Aqp4 was highly expressed in one subgroup and expressed at low levels in the other subgroup (Figure 2B). Therefore, these subpopulations were named Aqp4^{hi} and Aqp4^{lo} cells, respectively. Aqp4^{hi} cells excrete water from the retina through high expression of *Aqp4*. Although both subgroups expressed transglutaminase (*Glul*), Aqp4^{hi} cells had a higher expression of the glutamate-aspartate transporter (*Slc1a3*), suggesting a stronger ability to transport glutamate (Figure 2C). Aqp4^{hi} cells rapidly hydrate large amounts of carbon dioxide produced by photoreceptor metabolism into bicarbonate and protons outside of the retina via carbonic anhydrase XIV (*Car14*) on the cell membrane(27). In addition, the adhesion molecule Ncam1 that contacts nerve cells and the connexin Cdh5 that contacts endothelial cells are also highly expressed on Aqp4^{hi} cells. In addition, Aqp4^{hi} cells highly expresses transcription factors of the Ap-1 family (*Jun, Junb, Fos*). The AP-1 family has been proven to affect a variety of cellular processes (such as differentiation, proliferation, and apoptosis), depending on the cellular environment and stimuli(28). This means that Aqp4^{hi} cells are prone to phenotypic changes caused by environmental changes. The above enzymes and proteins are rarely expressed in Aqp4^{lo} cells. The above evidence indicates that Aqp4^{hi} cells are closely related to blood vessels and nerves and are the classic Müller cell type reported in previous studies; these cells are of great significance for maintaining homeostasis of the retinal environment.

Interestingly, a phototransduction process similar to that of photoreceptors was observed in Aqp4^{lo} cells: retinal and opsin combine to form rhodopsin, which activates the transduction protein when rhodopsin absorbs light(29). Transducins in turn activate phosphodiesterase, reduce cGMP levels and regulate downstream ion channels. Recent research showed that in addition to rods and cones, intrinsically photosensitive retinal ganglion cells (ipRGCs) can directly transduce light signals(30). Although Aqp4^{lo}

cells express components of the phototransduction pathway, because the downstream neurons are not yet clear, we still cannot prove that Müller cells becomes a new type of photoreceptor cell. Notably, multiple studies have shown that in the absence of photoreceptors, Müller cells express components of the photoreceptor pathway to replenish and replace missing photoreceptors. For example, in a mouse model of retinitis pigmentosa (RP), the expression of genes in pathways involved in the maintenance of photoreceptors in Müller cells was significantly increased with the loss of rods and cones(31). Similarly, M. Goel et al. observed the expression of rhodopsin in Müller cells in mice with inherited retinal degeneration (RD)(32). Although it cannot be demonstrated that Aqp4^{lo} cells are a class of photoreceptors other than rods and cones, our study confirms the existence of a subclass of Müller cells expressing photoreceptors in the normal retina. Furthermore, we believe that Aqp4^{lo} cells are the Müller cells that compensate for photoreceptors in diseases involving photoreceptor degeneration. In conclusion, the role of Aqp4^{lo} cells in normal and diseased retinas deserves further exploration.

Genomic variation analysis (GSVA) was performed on these two groups of cells, and the limma package was used to calculate the differential pathways of the two groups of cells (Figure 2D)(33). The Notch and Wnt signaling pathways were significantly enriched in Aqp4^{hi} cells. A previous study confirmed that these studies can be activated by retinal damage to cause Müller cell proliferation(34, 35).

2.2.2 Cellular communication of Aqp4^{hi} and Aqp4^{lo} cells in the NVU

We describe the communication signaling pathway of the NVU structure in terms of "cell–cell contact" and "secretory signaling". Aqp4^{hi} cells, RGCs, and astrocytes mediate cell-to-cell contact via cell adhesion molecule (CADM), cadherin (CDH), and neural cell adhesion molecule (NCAM) (Figure 2E, S2E and S3B). Astrocytes secrete a variety of signaling factors (vascular endothelial growth factor (VEGF), Midkine, and Pleiotrophin) that act on other cells in the NVU. Both astrocytes and RGCs secrete VEGF, which acts on endothelial cells and Aqp4^{hi} cells to regulate their function. However, astrocytes mainly secrete vegfa, while RGCs mainly secrete vegfb. Analysis of intracellular communication within the NVU suggests the following: 1) Aqp4^{hi} cells and astrocytes encapsulate RGCs to form a glial barrier, and this close contact explains the rapid onset of reactive gliosis following RGC axonal injury(36). 2) Astrocytes are the core of signal secretion in the NVU, which is beneficial for maintaining the normal function of blood vessels and neurons. 3) Aqp4^{lo} cells are rarely involved in cellular communication with other cells in the NVU, possibly to maintain their photoconductive properties.

2.2.3 Transcriptional regulatory mechanisms underlying the distinct phenotypes of the two Müller cell subpopulations

We then used SCENIC to infer the transcription factor (TF) regulatory information underlying the different phenotypes of the two Müller cell subclusters (Figure 2F and 2G)(37). Aqp4^{lo} cells highly express Neurod1 to regulate photoreceptor genes (*Gnat*, *Nrl*). Aqp4^{hi} cells express Pax6, Sox9, and Dbp to regulate

adhesion factors, glutamate transport, and carbon dioxide uptake. Id1 regulates the metabolic function of Aqp4^{hi} cells. Jund regulates other AP-1 family members.

2.2.4 Verification of the existence of two Müller cell subgroups

To verify the accuracy of the Müller cell subcluster clustering, we integrated Müller cells into the P14 samples and our analysis samples using canonical correlation analysis (CCA)(38). After regrouping the integrated data, five cell subclusters were obtained, of which cluster_0 and cluster_1 accounted for the main portion of the cells. Cluster_0 and cluster_1 correspond to Aqp4^{hi} and Aqp4^{lo} cells, respectively (Figure 2H and 2I). Based on the integrated data, we identified markers for Müller cell subclusters (Figure 2J). In conclusion, we identified and validated two specific Müller cell subclusters in the retina and further explored their phenotypic differences and underlying transcriptional mechanisms.

2.3 Phenotypic changes and underlying mechanisms of the NVU in two models

2.3.1 Müller_EAU cells are differentiated from Aqp4^{hi} cells

Next, we investigated the phenotypic changes and underlying mechanisms of the NVU in AireKO and NdpKO mice. In addition to Aqp4^{hi} and Aqp4^{lo} cells, there is a specific group of Müller cells that exist only in AireKO and are named Müller_EAU. Correlations among the three Müller cell subgroups calculated using conserved genes of Müller cells indicate that the gene expression patterns of Aqp4^{hi} and Müller_EAU cells are highly similar (Figure 3A). Meanwhile, Müller_EAU cells do not express photoreceptor genes. Furthermore, pseudotime analysis of the three subgroups confirmed that Müller_EAU cells are derived from the differentiation of Aqp4^{hi} cells (Figure 3B). Therefore, we believe that intense inflammation of the retina in AireKO mice drives the phenotypic changes of Aqp4hi cells and converts them to Müller_EAU cells.

2.3.2 Phenotypic transition of Müller cells and astrocytes in AireKO mice

We next investigated the cells with the most significant DEGs in AireKO Müller cells and astrocytes (Figure 3C). We noticed that the guanylate-binding protein family (Gbp), proteasome B-type family (Psmb), and interferon-inducible protein (Ifi) were all upregulated, which was confirmed to be induced by interferon(39, 40). In addition, astrocytes specifically upregulated complement genes. GSVA showed that astrocytes and Müller_EAU cells significantly upregulated inflammatory pathways(33), of which the JAK/STAT pathway may be an important mechanism for regulating inflammation in both cell types (Figure 3D). Notably, both Müller cells and astrocytes downregulated the Notch pathway. Studies

have shown that the downregulation of the Notch pathway is related to Müller cell dedifferentiation(41); however, the specific mechanism remains to be further studied. Biosynthesis of pantothenic acid and coenzyme A, which are important intermediates in cellular energy metabolism, is reduced in astrocytes and Müller cells. The former can also increase glutathione biosynthesis to slow apoptosis and cell damage(42), suggesting that the antioxidative stress capacity of glial cells is attenuated in AireKO mice.

2.3.3 Transcriptional mechanisms underlying the phenotypic transition of Müller cells and astrocytes

SCENIC analysis showed that Müller cells mainly upregulated three types of transcription factors: 1) the AP-1 family (*Fos, Jun, Junb, Fosb*); 2) Stats (*Stat1, Stat2, Stat3*); and 3) the interferon regulator family (*Irf1, Irf2*) (Figure 3E). The expression of Irf family members in Müller cells confirmed that the degeneration of Müller cells is directly affected by IFN-γ secreted by Th1 cells. Although astrocytes also upregulate members of the Stat and Irf families of transcription factors, they rarely express members of the AP-1 family, suggesting that AP-1 may play an important role in the phenotypic changes of only Müller cells. Astrocytes also upregulate Cebpb and the cAMP response element modulator Crem in AireKO mice to regulate immune inflammatory responses(43, 44). Downregulation of Id1 in astrocytes is associated with attenuation of self-renewal and differentiation processes(45).

SCENIC provided regulatory predictions for three classes of transcription factors (Figure 3F and S2F). The Stat family and Irf family regulate MHC-II genes and proteasomes (Psmb8 and Psmb9), among which Stat1 and Irf8 also promote the expression of interferon-inducible proteins. The network diagram indicates that Stat1 and Irf8 are the main regulators in the Stat and Irf family. Transcription factors such as the AP-1 family, Atf3, and Egr1 can also promote the release of some chemokines; however, the inflammation of Müller_EAU cells may be mainly affected by the Stat and Irf family. Notably, some genes regulated by *Fos* and *Junb* were highly expressed in normal Aqp4^{hi} cells but significantly downregulated in cells from AireKO mice. We believe that the loss-of-function of Müller_EAU cells may be closely related to the Ap-1 family; however, the specific mechanism deserves further exploration.

2.3.4 Phenotypic transition of Müller cells in NdpKO mice

We investigated DEGs in NdpKO mice for all subclusters within the NVU (Figure 3G). Both Müller cell subgroups upregulated NADH dehydrogenase-related genes. Aqp4^{hi} cells also upregulated *Vegfa* to induce neovascularization, which did not occur in Aqp4^{lo} cells. Gene Set Enrichment Analysis (GSEA) results also confirmed the metabolic shift of Aqp4^{hi} cells: glycolysis and oxidative phosphorylation pathways were upregulated (Figure 3H).

Endothelial cells showed impaired glucose uptake in NdpKO mice, as indicated by downregulation of multiple glucose transporters and upregulation of the lipoprotein lipase (LPL) transporter. Notably, endothelial cell-secreted basement membrane (BM) components (collagen IV and Lamin proteins) were

upregulated (Figure 3G and S3C), confirming thickening of the basement membrane in the microvasculature in NdpKO mice, which impairs intercellular communication, reducing barrier function(46). Meanwhile, downregulation of claudin proteins (*Ocln, Lsr, Pltp*) revealed impaired tight junctions between endothelial cells (Figure 3G). Thickening of the basement membrane, together with disruption of tight junctions, suggests damage to the endothelial barrier, while other cells show only altered metabolism (Figure S3D). Therefore, we speculate that endothelial barrier disruption is the first pathological change in NdpKO mice, and $Aqp4^{hi}$ cells respond to this change by secreting proangiogenic factors to alleviate the hypoxic environment.

2.3.5 Transcriptional mechanisms of endothelial barrier impairment

To investigate the mechanism of endothelial barrier disruption, we further investigated the transcriptional mechanism and gene regulatory network of endothelial cells in NdpKO mice (Figure 3I and S3E). SCENIC analysis revealed activation of the transcription factors *Ets1* and *Mef2c*, whose target genes (*Dlc1, Nrp, Plvap*) were upregulated in NdpKO cells and were verified to play an important role in the regulation of angiogenesis and the formation of polarized structures(47-49). On the other hand, the forkhead box (*Fox*) family (*Foxf2, Foxp1, Foxq1*) and *Lef1* and its downstream target genes were all downregulated in NdpKO mice. Gene regulatory networks revealed that FOX genes and *Lef1* regulate adhesion proteins (*Ocln, Lsr, Pltp*) and downregulate glucose transporters and extracellular matrix (ECM) components, which reveals the mechanism of endothelial barrier impairment(50, 51).

2.4 Infiltration of T cells in AireKO mice

2.4.1 Subpopulations of T cells in AireKO mice

Abundant lymphocytes infiltrate the retina of mice with EAU(52), among which Th1 cells are the main cells driving inflammation, mobilizing other immune cells by secreting IFN-γ(53, 54). NK and $CD8^+$ T cells are among the most important pathogenic factors of Bechtel uveitis (BU): the active phase of BU is dominated by $CD8^+$ T- and NK-cell infiltration, while other types of uveitis are dominated by $CD4^+$ T cells(55). Since T cells and NK cells were identified as the same cluster, we regrouped this cluster to obtain NK cells, Treg cells, $CD8^+$ T cells, and helper T cells (Th cells) (Figure 4A). Th cells included one Th0 subpopulation and three Th1 subpopulations. We identified markers for three subgroups and renamed them accordingly: *Ifng*$^+$ T, *Sostdc1*$^+$ T and *Il10*$^+$ T cells (Figure S4A and S4B).

The pie chart shows that the severity of EAU is closely related to the degree of immune cell infiltration (Figure 4B). According to the dendrogram of the genes of each subgroup, *Il10*$^+$ T cells were more similar to *Ifng*$^+$ T cells, while *Sostdc1*$^+$ T cells were more similar to Th0 cells (Figure 4B).

2.4.2 Inflammatory factors secreted by T and NK cells

We investigated the expression of different classes of inflammatory mediators in these immune cells. As the most important inflammatory mediator mediating retinal inflammation in uveitis, IFN-γ is mainly secreted by *Ifng*$^+$ T cells (Figure 4C). In addition, *Ifng*$^+$ T cells secrete a variety of chemokines that drive inflammation and tissue damage. Therefore, we consider *Ifng*$^+$ T cells to be the main proinflammatory cells. *Il10*$^+$ T cells, on the one hand, can secrete some inflammatory factors, like Th1 cells, to exert proinflammatory effects, and on the other hand, they can also secrete Il10 and TGFβ1 to exert anti-inflammatory effects. The release of Il10 has been confirmed to have a clear inhibitory effect on uveitis(56, 57). In contrast to *Ifng*$^+$ T cells, *Sostdc1*$^+$ T cells secreted fewer inflammatory factors and were phenotypically similar to Th0 cells, which may be undifferentiated Th1 cells. Compared with *Ifng*$^+$ T and *Il10*$^+$ T cells, *Sostdc1*$^+$ T cells secreted the fewest inflammatory factors and had phenotypes similar to those of Th0 cells, which may be undifferentiated Th1 cells. NK and CD8$^+$ T cells not only secreted chemokines (*Xcl1* and *CCL3*) but also secreted granzyme, which induces programmed death in target cells. The cytotoxic effects of NK cells and CD8$^+$ T cells may be an important reason why BU is more recurrent and destructive than other forms of uveitis. In addition, we observed that *Ifng*$^+$ T cells also secrete proteins that regulate cytotoxic granules (*Nkg7, Lgals1*)(58, 59), indicating a cytotoxic effect. In uveitis, Treg cells are the main anti-inflammatory cells in the retina(60). Here, we observed that Treg cells significantly upregulated a variety of cellular receptors regulated by a variety of inflammatory factors secreted by humoral and intraretinal immune cells.

Kyoto Encyclopedia of Genes and Genomes (KEGG)(61) enrichment analysis was performed on NK- and T-cell subsets, and the enriched pathways were divided into four categories (Figure 4D). *Ifng*$^+$ T and NK cells were significantly enriched in adhesion- and migration-related pathways. The Rap1, NF-κB and JAK-STAT signaling pathways were enriched in all five types of cells and are closely related to the regulation of inflammation in these cells.

2.4.3 Transcriptional mechanisms regulating T- and NK-cell inflammation

SCENIC analysis revealed that the transcription factors *Runx2*, *Stat3* and *Ets1* were significantly activated in *Ifng*$^+$ T cells (Figure 4E). Gene regulatory networks (GRNs) revealed their downstream inflammatory mediators (Figure 4F and S4C). NK cells upregulate *Eomes* to regulate the killer cell lectin-like receptor, which is the basis for the cytotoxic effect of NK cells(59). They also upregulate *Irf8*, which regulates the expression of chemokines and receptors. Simultaneous activation of *Runx3* in NK cells and *Ifng*$^+$ T cells can promote the encoding and release of granzymes, which may be a common mechanism by which the two cell types exert cytotoxicity (Figure 4G). As one of the target genes of *Maf*, *Il10* is specifically expressed in *Il10*$^+$ T cells (Figure 4G). Therefore, Maf may become an important target for inducing Th1 cells to secrete *Il10*.

2.5 Monocytes and their derived cells in AireKO mice

The infiltration of $CD4^+$ T cells in autoimmune uveitis is dependent on the activation of antigen-presenting cells (APCs). Studies have demonstrated that preventing the recruitment and/or maturation of APCs largely inhibits the generation of antigen-specific T cells(62-64).

2.5.1 MO-MA lineages, MO-DC lineages and microglia

In uveitis, monocytes (MO) in the peripheral blood are recruited to cross the BRB and differentiate into macrophages (MA) and dendritic cells (DC). In our samples, monocytes and their derived cells and microglia were mixed and aggregated into one cluster. We regrouped the cluster and obtained MO-MA lineages, MO-DC lineages and microglia according to canonical markers(65, 66) (Figure 5A).

Since macrophages and microglia exhibit similar gene expression patterns under the pathological condition of uveitis, it is difficult to distinguish them. Here, we can better differentiate mature APCs in the retina by multiple gene markers (Figure 5B).

2.5.2 Pseudotime trajectories of MO-DC lineags

We constructed a pseudotime trajectory of MO-DC lineages and divided them into monocytes with DC differentiation potential (Monocyte_DC), dendritic cell-committed monocytes (DC-committed Mo) and two mature dendritic cells: conventional DCs (cDCs) and plasmacytoid DCs (pDCs) (Figure S5A and S5B).

GeneSwitches were utilized for the MO-pDC differentiation trajectories(67), and we defined the transitions of key transcription factors along the trajectory and the order in which these transitions occurred (Figure 5C and S5C). Activation of the transcription factor *Bcl11a*, an early switching event on the pDC differentiation trajectory, has been shown to be an essential lineage change regulating pDC development(68). The transcription factors *Runx2*, *Hoxa7*, *Spib*, and *Cxxc5* are subsequently activated and maintain differentiation into pDCs.

Next, we compared the phenotypic differences between cDCs and pDCs (Figure 5D). We found that many MHC-II genes and costimulatory molecules (CD80, CD86, CD40) were upregulated along the trajectory from Monocyte_DC to cDCs, revealing the gradually enhanced antigen processing and presentation ability of these cells. The high expression of actin, myosin and integrin family genes in cDCs is related to chemotaxis. We observed that the expression levels of Nfkbia and the P100/RelB dimer (Nfkb2/Relb) were all significantly elevated in cDCs. The former is a key complex in the classical NF-kB signaling pathway, and the latter is a key nuclear transcription factor in the noncanonical pathway(69). This evidence suggests that the simultaneous activation of the canonical and noncanonical NF-kB signaling pathways is an important mechanism for the differentiation and maturation of cDCs in EAU. In contrast to cDCs, pDCs downregulate inflammatory factors and adhesion proteins along the differentiation

trajectory from Monocyte_DC to pDCs. Interestingly, the IFN-α receptor is highly expressed in pDCs, suggesting that their differentiation may be induced by IFN-α.

2.5.3 Pseudotime trajectories of MO-MA lineags

Likewise, we divided MO-MA lineages into monocytes with macrophage differentiation potential (Monocyte_ma), macrophage-committed monocytes (ma_committed mo), and mature macrophages (macrophages) (Figure 5E, 5F and S5D). From Monocyte_ma to macrophages, secreted inflammatory factors changed: Ccl6, Ccl9, and Il1β were downregulated, while Ccl3, Ccl4, and cathepsin D (Ctsd) were upregulated (Figure 5G and S5E).

2.5.4 Microglia in AireKO mice

Microglia are activated to exert inflammatory effects under pathological conditions(70). Here, by comparing microglia and monocyte-derived macrophages in EAU, we found that macrophages highly expressed a variety of chemokines, and their inflammatory effects were strong. This finding suggests that peripheral blood-derived macrophages, rather than microglia, are the main pathogenic macrophages in EAU (Figure 5H and S5F).

2.6 Immune regulatory network in AireKO mice

We paid particular attention to the inflammatory regulatory network mediated by immune infiltrating cells in AireKO mice. Therefore, we performed an in-depth dissection of the regulatory networks among inflammatory cells and between inflammatory cells and cells in the NVU.

2.6.1 Regulatory network among infiltrating immune cells

Interestingly, we noticed that monocytes (including Monocyte_DC and Monocyte_MA) are stimulated by a variety of inflammatory factors: 1) almost all immune cells secrete Ccl5 to act on monocytes; 2) *Ifng*$^+$ T and macrophages secrete Ccl3 and Ccl4 to act on monocytes; 3) *Ifng*$^+$ T secrete IFN-γ to act on monocytes; 4) MO-MA lineages act on monocytes, with Monocyte_MA secreting Ccl8 to act on two monocyte subclasses and macrophages secreting Ccl2 and Ccl12 to act on Monocyte_DC; and 5) Monocyte_DC secretes Ccl6 and Ccl9 to act on two monocyte subclasses (Figure 5I and 5J).

These results suggest that the inflammatory environment in AireKO mice induces monocytes to convert to DCs or macrophages and activate *Ifng*$^+$ T cells through antigen presentation. Therefore, a closed loop of "inflammatory cell - monocyte - APC - *Ifng*$^+$ T cells" is formed to produce an inflammatory cascade.

Monocytes and their derived cells act directly on the T-cell population by secreting Cxcl16, which can enhance cytotoxicity and induce higher levels of IFN-γ secretion(71). Macrophages are regulated by other

immune cells due to the expression of Ccr5. NK cells are regulated by two subclasses of monocytes and macrophages via expression of Ccr2.

2.6.2 Regulatory network between inflammatory cells and cells in the NVU

It is worth noting that almost all cell subsets in the NVU upregulate MHC-II genes and secrete inflammatory factors, thus becoming key links in the inflammatory network. Similar to the previous results, all cells in the NVU act on monocytes (Figure 5K): 1) Müller_EAU and astrocytes secrete Ccl5 and Ccl8, and astrocytes also specifically release complement; 2) endothelial cells secrete Galectin-9 (Igals9); 3) RGCs release Ccl27a; and 4) pericytes release Il34. Inflammatory mediators secreted by cells in the NVU differ from infiltrating immune cells, but they both promote monocyte maturation and induce chemotaxis, adhesion, and migration.

2.6.3 Impairment of cellular normal regulatory networks in the NVU

In summary, immune cells and cells in the NVU together constitute an closed inflammatory loop of "inflammatory cells/NVU - monocytes - APC - *Ifng*$^{+}$ T cells". Therefore, blocking the induction of monocytes by inflammatory cells and/or cells in the NVU can block the progression of inflammation and may become a new direction for the treatment of autoimmune uveitis in the future.

Furthermore, we found that cellular self-protection signaling is impaired in the NVU. The expression levels of brain-derived neurotrophic factor (BDNF) and VEGF secreted by astrocytes were decreased (Figure 5K), suggesting that the neuroprotective effect of astrocytes on RGCs and the ability to maintain vascular integrity were weakened(72).

3 Discussion

The NVU is the basic functional unit of nutrition and metabolism in the retina, and the destruction of its structure is an important risk factor for the development and progression of retinal diseases. Alleviating NVU damage is an urgent need for the treatment of retinal diseases. However, recent research on NVU injury has often focused on a certain type of disease, ignoring the common pathological features among diseases. In addition, research on retinal diseases has typically focused on the changes of a single component within the NVU rather than the overall structure, and systematic analysis of the mechanism of NVU damage is lacking. Therefore, multidisease analysis based on scRNA sequencing was applied to the mouse retina, which explored the cellular and molecular mechanisms of NVU injury from a broader perspective and provided a rationale for exploring common therapeutic targets for multiple diseases. We integrated ScRNA sequencing data from the retinas of WT, AireKO, and NdpKO mice, which clinically manifested as normal, EAU, and FEVR. EAU and FEVR correspond to retinal inflammation and hypoxia, pathological processes common to almost all retinal diseases. Our study deciphers the specific

degeneration mechanisms of the NVU under inflammatory and hypoxic conditions, providing therapeutic targets for EAU and FEVR. Our exploration of the common mechanisms of NVU injury in multiple diseases provides profound insights into approaches to prevent further deterioration in various retinal diseases.

We constructed a single-cell atlas of the entire retina. We examined the specific gene markers of different cell types in the retina and used another mouse retinal single-cell sample, P14, to verify the accuracy of these markers, which provided a basis for the subsequent identification of retinal cell types. In the retina, NVU structures displayed strong intercellular communication signals, and alterations in the NVU were predominant in both pathological models.

We identified and validated two subclusters of Müller cells, Aqp4^{hi} and Apq4^{lo} cells. As classic Müller cells, Aqp4^{hi} cells are more important than Aqp4^{lo} cells in metabolizing neurotransmitters, maintaining neuronal ionic environment stability and water metabolism, transporting carbon dioxide, and participating in the BRB. However, Aqp4^{lo} cells express genes in the phototransduction pathway, such as rhodopsin and phosphodiesterase (Fig. 6, upper left). M Goel and Yohei Tomita detected compensatory expression of rhodopsin by Müller cells to replace photoreceptor function in two separate studies of diseases with photoreceptor degeneration(31, 32). Here, we found that a small group of Müller cells express photoreceptor genes in the normal retina. Therefore, we speculate that the specific Müller cells found in that previous study were derived from Aqp4^{lo} cells. To verify the accuracy of our conclusions, we also integrated Müller cells in P14 samples to expand the total number of cells. After reclustering, two main subgroups, classical Müller cells and photosensitive Müller cells, can still be obtained. Combining the three samples, we present a detailed list of specific markers to identify Müller cell subgroups, providing a theoretical basis for subsequent exploration.

We explored the transcriptional mechanisms regulating the functions and predicting the positional relationships of these cells in the retina. The complex functions of Aqp4^{hi} cells are regulated by multiple transcription factors: *Sox9* regulates water homeostasis, *Dbp* regulates glutamate transport, etc. Markers of neural progenitor cells or stem cell properties, such as *Pax6* and *Hes1*, are highly expressed in Aqp4^{hi} cells, suggesting the potential of these cells to transform into pluripotent stem cells or retinal progenitor cells(73, 74). In Aqp4^{lo} cells, *Neurod1* regulates the expression of photoreceptor genes. Therefore, targeting Neurod1 with Aqp4^{lo} cells as a carrier is expected to realize the possibility of replacing photoreceptors with Müller cells. In addition to differences in phenotype, we believe that there are also significant differences in positional relationships between the two cells subgroups in the retina. 1) Aqp4^{hi} cells are more abundant at sites of cellular communication with other structures of the NVU, and 2) Aqp4^{hi} cells express aquaporin and carbonic anhydrase, which are distributed on the interface between glial cells and endothelial cells to promote the redistribution of water from retinal tissue into the blood. 3) Aqp4^{hi} cells highly express neural cell adhesion molecules. The above evidence indicates that Aqp4^{hi} cells are more closely related to the microvascular system and neurons and play a more important role in the maintenance of the NVU structure. In conclusion, we believe that Aqp4^{hi} cells are more important for

DR, glaucoma and other diseases with damaged vascular barriers and/or neuronal degeneration, while Aqp4^{lo} cells are more important for diseases with photoreceptor deletion, such as RP.

We investigated major changes in the NVU in EAU and FEVR mouse models; the former is dominated by degeneration of Aqp4^{hi} cells, and the latter is dominated by changes in endothelial cells and Aqp4^{hi} cells. In EAU, a large number of immune cells infiltrate the retina, resulting in severe damage to the NVU structure. Although all cells in the NVU were significantly altered, Müller cells were the most prominent. There is a cluster of Müller cells that exists only in EAU: Müller_EAU. Since the number and location of Müller cells in mature mice are basically unchanged, combined with the similarity in gene expression, we believe that Müller_EAU is derived from Aqp4^{hi} cells. The inflammatory environment promotes the phenotypic changes of Aqp4^{hi} cells, manifested as dysfunction of the transport of water, carbon dioxide, glutamate, etc., which triggers disruption of the retinal internal environment and aggravates neuronal apoptosis. Meanwhile, Müller_EAU can also secrete inflammatory mediators to promote the infiltration of immune cells.

The changes in Aqp4^{hi} cells are regulated by three types of transcription factors: the Irf family, Stat family, and Ap-1 family (Fig. 6, upper right). Inhibiting the transcription of these three families will be beneficial to inhibit or delay or even reverse the degeneration of Müller cells. In FEVR, the retina exhibits a hypoxic environment, with the earliest changes being increased BRB permeability and leakage of substances in the blood (Fig. 6, bottom left). We found that the tight junctions of endothelial cells were disrupted and that increased basement membrane proteins secreted by endothelial cells resulted in thickening of the basement membrane. Changes in endothelial cells are affected by the Fox family. In addition to endothelial changes, Aqp4^{hi} cells also upregulate VEGF secretion to promote neovascularization.

In EAU, infiltration of immune cells is a prerequisite for NVU injury. T lymphocytes, NK cells, and mononuclear lineages infiltrating the retina became the focus of our study. *Ifng*$^{+}$ T cells are the most proinflammatory T cells and are central to the pathogenesis of EAU. The cytotoxic effects of NK cells and *Ifng*$^{+}$ T cells on neuronal damage may better explain the more destructive effects of Behçet's uveitis compared to other types of uveitis. There is a cluster of Th1 cells that can secrete Il10 and is regulated by the transcription factor *Maf*, which exerts some degree of anti-inflammatory effects. Monocytes include two types of monocytes with different differentiation potentials: one differentiates into DCs (including cDCs and pDCs), and the other differentiates into macrophages. We also investigated the regulatory mechanisms of differentiation trajectories, providing new insights into the inhibition of monocyte maturation. By studying cellular crosstalk in EAU, we found that both monocytes were strongly induced by chemokines secreted predominantly by immune cells and cells in the NVU. After maturation, monocytes transform into antigen-presenting cells and stimulate the activation of *Ifng*$^{+}$ T cells, resulting in the amplification of the inflammatory cascade. A closed loop of "inflammatory cells/NVU - monocytes - APC - *Ifng*$^{+}$ T cells" is formed (Fig. 6, bottom right). Blocking the effect of inflammatory mediators on monocytes or inhibiting monocyte maturation may be the main way to break the closed loop.

In conclusion, this study systematically investigated the complexities of the NVU in inflammatory and hypoxic environments. Our results emphasize the importance of a newly identified group of Müller cells, $Aqp4^{hi}$ cells, in specific degeneration mechanisms in different diseases. Our integrative analysis provides unparalleled insight into NVU heterogeneity in different types of retinal diseases, advancing our understanding of the pathogenesis of multiple diseases. It opens up more possibilities for developing novel targeted drugs with greater precision to block disease progression due to NVU damage and provides a reference for the many scientists interested in this topic.

4 Methods

Data source and acquisition

Single-cell transcriptome files of samples from GSE132229 and GSE125708 were downloaded from the Gene Expression Omnibus (GEO) database (http://www.ncbi.nlm.nih.gov/geo/) to be used in our research, including 4 AireKO samples, 2 NdpKO samples and 6 WT samples. To validate our conclusion, another sample from GSE63473, including 7 WT samples, was downloaded from the GEO database. The study utilized publicly available datasets with preexisting ethics approval from the original studies. Informed consent was obtained from each participant.

Processing of single-cell RNA-seq data

The generated UMI count matrices for the samples were loaded sequentially into R using the Read10X function of Seurat (http://satijalab.org/seurat/, R package)(38). After adding the sample information in the row names of the matrices, all of the data were merged, and the Seurat object was created. Then, the data were filtered and normalized. Specifically, cells were retained with 400 < nFeature_RNA < 7000, percent.mt < 20 and percent.rp < 20. Finally, 61,953 cells passed the quality filter, of which 21,469 were from AireKO model mice, 10,218 were from NdpKO model mice, and 30,266 were from wild-type mice. We used the FindClusters() function to perform clustering (resolution=1.2) and UMAP plots for visualization. For normalized gene expression data, we used the FindAllMarkers function to list the markers of each cell cluster. Compared with that in other cells, the expression of these marker genes was higher than log2(1.5). The main cell types were identified based on our own findings and markers described in the original literature.

Quality control and normalization of P14 samples were similar to those described above. The final 31,604 cells were used for subsequent validation analysis, and we performed unbiased clustering on the data to obtain 58 cell clusters. Except for resolution = 2, the methods for cell clustering and identification were the same as those described above.

Gene enrichment analysis

The FindMarkers function was used to identify DEGs between two clusters (adjusted p value <0.01 and fold change [FC] >1.5). The R package clusterProfiler(75) was used to perform GO(76) and Kyoto Encyclopedia of Genes and Genomes (KEGG)(61) pathway enrichment for the DEGs. Based on the gene set data for *Mus musculus* in the msigdbr package (selections: C2 for category and CP: KEGG for subcategory), we used GSEA to identify gene sets that were significantly enriched in specific cell clusters(77). We limited the threshold to a false discovery rate (FDR) q-value <0.25 and a p value <0.1.

GSVA was performed using the same gene set used for GSEA to analyze the enriched gene sets between different cell subtypes(33). Subsequently, the limma package was used to determine the gene sets with significant differences(78). Differentially enriched signatures were defined as having FDR adjusted p values < 0.05 and |mean score difference| values ≥ 0.1, as described previously. Then, the pheatmap() function in the package pheatmap (1.0.12) was used to render the results as heatmaps.

Pseudotime analysis

To understand the transitions between certain cells, trajectory analysis was conducted using Monocle2(79). We used FindConservedMarkers() to find markers that were conserved among groups and then used these genes for subsequent analysis. The analysis used the newCellDataSet() function to create a monocle object from clustering analysis. After reducing the dimensionality of the data through the reduceDimension() function, the cells were ordered along pseudotime. The function plot_cell_trajectory() was used to generate plots of pseudotime by state, cluster and pseudotime. Furthermore, we analyzed different genes related to pseudotime analyses through the differentialGeneTest() function. The heatmap of clusters along the pseudotime trajectory was also generated using the plot_pseudotime_heatmap() function.

According to the results of Monocle2 analysis, the genes were divided into different patterns, and each pattern was then subjected to KEGG enrichment analyses.

Using GeneSwitches(67), we first performed binarization analysis of genes along the differentiation trajectory and screened out potential switch genes with on and off states in their expression characteristics. Then, we performed logistic regression analysis and pseudotime correlation analysis of these potential switch genes to obtain the R value of each correlation. A stronger pseudochronological correlation was associated with a closer relationship between the gene and the trajectory process. After obtaining the switch time and the correlation R value of each potential switch gene, the top switch genes were sorted and visualized in pseudochronological order according to their switch times. We also used GeneSwitches to obtain the enrichment analysis results for switch genes through gene annotation (such as surface proteins, transcription factors and other functional types).

Cell–cell interaction analysis

To visualize and analyze intercellular communications from our data, we conducted CellChat analysis(23). We create a new CellChat object from our Seurat object. The cell types were added to the CellChat object as cell metadata. CellChat identified differentially overexpressed ligands and receptors for each cell group and associated each interaction with a probability value to quantify communications between the two cell groups mediated by these signaling genes. Significant interactions were identified on the basis of a statistical test that randomly permuted the group labels of cells and then recalculated the interaction probability. The results were visualized using bubble and chordal plots through the netVisual_bubble() and chordDiagram() functions. Furthermore, we identified and visualized outgoing and incoming communication patterns of cells using the identify CommunicationPatterns() functions.

SCENIC analysis

SCENIC is a computational method for simultaneous gene regulatory network reconstruction and cell-state identification from single-cell RNA-seq data (http://scenic.aertslab.org)(37). We first obtained the scores of different TFs in cell subtypes through R and then screened according to the criteria of avg.exp ≥ 1, pct.exp ≥ 20 and RelativeActivity ≥ 1 to obtain important TFs. We obtained the target gene information of TFs using pyscenic and screened them with the same criteria. The input matrix used for pyscenic was the normalized expression matrix output from Seurat.

According to the expression of TFs and target genes and their importance, we visualized the results using the Cytoscape tool (version 3.8.2) (specific screening criteria are shown in the legend). The interactions of each TF and target were merged manually to analyze the overall interactions. We also visualized the target genes of several important TFs with a UMAP plot.

Abbreviations

NVU
Retinal neurovascular unit
DR
Diabetic retinopathy
ROP
Retinopathy of prematurity
EAU
Experimental autoimmune uveitis
FEVR
Familial exudative vitreoretinopathy
RVO
Retinal vascular occlusion
ScRNA-seq
Single-cell RNA sequencing

WT
Wild-type
BCs
Bipolar cells
HCs
Horizontal cells
ACs
Amacrine cells
RGCs
Retinal ganglion cells
BRB
The blood–retinal barrier
PVMs
Perivascular macrophages
DEGs
Differentially expressed genes
NMOSDs
Neuromyelitis optica spectrum disorders
DME
Diabetic macular edema
IpRGCs
Intrinsically photosensitive retinal ganglion cells
RP
Retinitis pigmentosa
RD
Inherited retinal degeneration
GSVA
Genomic variation analysis
TF
Transcription factor
CCA
Canonical correlation analysis
GSEA
Gene Set Enrichment Analysis
LPL
Lipoprotein lipase
BM
Basement membrane
BU
Bechtel uveitis

KEGG
Kyoto Encyclopedia of Genes and Genomes
GRNs
Gene regulatory networks
APCs
Antigen-presenting cells
MO
Monocytes
MA
Macrophages
DC
Dendritic cells
Monocyte_DC
monocytes with DC differentiation potential
DC-committed Mo
dendritic cell-committed monocytes
CDCs
conventional DCs
PDCs
plasmacytoid DCs

Declarations

Ethical Approval and Consent to participate

Not applicable

Consent for publication

Not applicable

Availability of data and materials

The dataset(s) supporting the conclusions of this article is(are) included within the article (and its additional file(s)).

Competing interests

The authors declare that the research was conducted in the absence of any commercial or financial relationships that could be construed as a potential conflict of interest.

Funding

Not applicable

Author's contributions

YZ, XY and XD performed the data analysis and constructed the datasets. XY, YZ and XD designed and generated the figures. YZ, XD and XY wrote the manuscript. MF, MC and GY supervised this project. All the authors reviewed and edited the manuscript.

Acknowledgments

All authors would like to thank the specimen donors and research groups for GSE132229, GSE125708 and GSE63473, which provided data for this article. We are grateful to Kaiwen Wang, Zhigui Wu and Jiao Jin for their advice on data processing and Chengliang Mao for his guidance in manuscript writing. We are also grateful to all members of this project for stimulating discussions during the preparation of this manuscript.

References

1. Hawkins BT, Davis TP. The blood-brain barrier/neurovascular unit in health and disease. PHARMACOL REV. [Journal Article; Research Support, N.I.H., Extramural; Research Support, Non-U.S. Gov't; Research Support, U.S. Gov't, P.H.S.; Review]. 2005 2005-06-01;57(2):173–85.
2. Hammes HP. Diabetic retinopathy: hyperglycaemia, oxidative stress and beyond. DIABETOLOGIA. [Journal Article; Review]. 2018 2018-01-01;61(1):29–38.
3. Meng C, Gu C, He S, Su T, Lhamo T, Draga D, et al. Pyroptosis in the Retinal Neurovascular Unit: New Insights Into Diabetic Retinopathy. FRONT IMMUNOL. [Journal Article; Research Support, Non-U.S. Gov't; Review]. 2021 2021-01-20;12:763092.
4. Ji L, Tian H, Webster KA, Li W. Neurovascular regulation in diabetic retinopathy and emerging therapies. CELL MOL LIFE SCI. [Journal Article; Review]. 2021 2021-08-01;78(16):5977–85.
5. Simo R, Stitt AW, Gardner TW. Neurodegeneration in diabetic retinopathy: does it really matter? DIABETOLOGIA. [Journal Article; Research Support, N.I.H., Extramural; Research Support, Non-U.S. Gov't; Review]. 2018 2018-09-01;61(9):1902–12.
6. Syc-Mazurek SB, Libby RT. Axon injury signaling and compartmentalized injury response in glaucoma. PROG RETIN EYE RES. [Journal Article; Research Support, N.I.H., Extramural; Research Support, Non-U.S. Gov't; Review]. 2019 2019-11-01;73:100769.
7. Tang F, Barbacioru C, Wang Y, Nordman E, Lee C, Xu N, et al. mRNA-Seq whole-transcriptome analysis of a single cell. NAT METHODS. [Journal Article; Research Support, Non-U.S. Gov't]. 2009 2009-05-01;6(5):377–82.
8. Heng JS, Hackett SF, Stein-O'Brien GL, Winer BL, Williams J, Goff LA, et al. Comprehensive analysis of a mouse model of spontaneous uveoretinitis using single-cell RNA sequencing. Proc Natl Acad Sci U S A. [Journal Article]. 2019 2019-12-16.

9. Heng JS, Rattner A, Stein-O'Brien GL, Winer BL, Jones BW, Vernon HJ, et al. Hypoxia tolerance in the Norrin-deficient retina and the chronically hypoxic brain studied at single-cell resolution. Proc Natl Acad Sci U S A. [Journal Article; Research Support, N.I.H., Extramural; Research Support, Non-U.S. Gov't; Research Support, U.S. Gov't, Non-P.H.S.]. 2019 2019-04-30;116(18):9103–14.
10. Masland RH. The fundamental plan of the retina. NAT NEUROSCI. [Journal Article; Review]. 2001 2001-09-01;4(9):877 – 86.
11. Lamb TD. Evolution of phototransduction, vertebrate photoreceptors and retina. PROG RETIN EYE RES. [Journal Article; Research Support, Non-U.S. Gov't; Review]. 2013 2013-09-01;36:52–119.
12. Hoon M, Okawa H, Della SL, Wong RO. Functional architecture of the retina: development and disease. PROG RETIN EYE RES. [Journal Article; Research Support, N.I.H., Extramural; Research Support, Non-U.S. Gov't; Review]. 2014 2014-09-01;42:44–84.
13. Yoo HS, Shanmugalingam U, Smith PD. Harnessing Astrocytes and Muller Glial Cells in the Retina for Survival and Regeneration of Retinal Ganglion Cells. CELLS-BASEL. [Journal Article; Review]. 2021 2021-05-28;10(6).
14. Mendes-Jorge L, Ramos D, Luppo M, Llombart C, Alexandre-Pires G, Nacher V, et al. Scavenger function of resident autofluorescent perivascular macrophages and their contribution to the maintenance of the blood-retinal barrier. Invest Ophthalmol Vis Sci. [Journal Article; Research Support, Non-U.S. Gov't]. 2009 2009-12-01;50(12):5997–6005.
15. Chen J, Qian H, Horai R, Chan CC, Falick Y, Caspi RR. Comparative analysis of induced vs. spontaneous models of autoimmune uveitis targeting the interphotoreceptor retinoid binding protein. PLOS ONE. [Comparative Study; Journal Article; Research Support, N.I.H., Extramural]. 2013 2013-01-20;8(8):e72161.
16. Xiao H, Tong Y, Zhu Y, Peng M. Familial Exudative Vitreoretinopathy-Related Disease-Causing Genes and Norrin/beta-Catenin Signal Pathway: Structure, Function, and Mutation Spectrums. J OPHTHALMOL. [Journal Article; Review]. 2019 2019-01-20;2019:5782536.
17. Gilmour DF. Familial exudative vitreoretinopathy and related retinopathies. Eye (Lond). [Journal Article; Research Support, Non-U.S. Gov't; Review]. 2015 2015-01-01;29(1):1–14.
18. Shekhar K, Lapan SW, Whitney IE, Tran NM, Macosko EZ, Kowalczyk M, et al. Comprehensive Classification of Retinal Bipolar Neurons by Single-Cell Transcriptomics. CELL. [Journal Article; Research Support, N.I.H., Extramural]. 2016 2016-08-25;166(5):1308–23.
19. Menon M, Mohammadi S, Davila-Velderrain J, Goods BA, Cadwell TD, Xing Y, et al. Single-cell transcriptomic atlas of the human retina identifies cell types associated with age-related macular degeneration. NAT COMMUN. [Journal Article; Research Support, N.I.H., Extramural]. 2019 2019-10-25;10(1):4902.
20. Shiwani HA, Elfaki MY, Memon D, Ali S, Aziz A, Egom EE. Updates on sphingolipids: Spotlight on retinopathy. BIOMED PHARMACOTHER. [Journal Article; Review]. 2021 2021-11-01;143:112197.
21. Macosko EZ, Basu A, Satija R, Nemesh J, Shekhar K, Goldman M, et al. Highly Parallel Genome-wide Expression Profiling of Individual Cells Using Nanoliter Droplets. CELL. [Journal Article; Research

Support, N.I.H., Extramural; Research Support, Non-U.S. Gov't; Research Support, U.S. Gov't, Non-P.H.S.]. 2015 2015-05-21;161(5):1202–14.

22. Wang Y, Liu Y, Fei A, Yu Z. LncRNA XIST facilitates hypoxia-induced myocardial cell injury through targeting miR-191-5p/TRAF3 axis. MOL CELL BIOCHEM. [Journal Article]. 2022 2022-06-01;477(6):1697–707.
23. Jin S, Guerrero-Juarez CF, Zhang L, Chang I, Ramos R, Kuan CH, et al. Inference and analysis of cell-cell communication using CellChat. NAT COMMUN. [Journal Article; Research Support, N.I.H., Extramural; Research Support, Non-U.S. Gov't; Research Support, U.S. Gov't, Non-P.H.S.]. 2021 2021-02-17;12(1):1088.
24. Fischbarg J. Water channels and their roles in some ocular tissues. MOL ASPECTS MED. [Journal Article; Research Support, Non-U.S. Gov't; Review]. 2012 2012-10-01;33(5–6):638 – 41.
25. Netti V, Fernandez J, Melamud L, Garcia-Miranda P, Di Giusto G, Ford P, et al. Aquaporin-4 Removal from the Plasma Membrane of Human Muller Cells by AQP4-IgG from Patients with Neuromyelitis Optica Induces Changes in Cell Volume Homeostasis: the First Step of Retinal Injury? MOL NEUROBIOL. [Journal Article]. 2021 2021-10-01;58(10):5178–93.
26. Kida T, Oku H, Horie T, Fukumoto M, Okuda Y, Morishita S, et al. Implication of VEGF and aquaporin 4 mediating Muller cell swelling to diabetic retinal edema. Graefes Arch Clin Exp Ophthalmol. [Journal Article]. 2017 2017-06-01;255(6):1149–57.
27. Reichenbach A, Bringmann A. New functions of Muller cells. GLIA. [Journal Article; Research Support, Non-U.S. Gov't; Review]. 2013 2013-05-01;61(5):651–78.
28. Lambuk L, Iezhitsa I, Agarwal R, Agarwal P, Peresypkina A, Pobeda A, et al. Magnesium acetyltaurate prevents retinal damage and visual impairment in rats through suppression of NMDA-induced upregulation of NF-kappaB, p53 and AP-1 (c-Jun/c-Fos). NEURAL REGEN RES. [Journal Article]. 2021 2021-11-01;16(11):2330–44.
29. Ebrey T, Koutalos Y. Vertebrate photoreceptors. PROG RETIN EYE RES. [Journal Article; Review]. 2001 2001-01-01;20(1):49–94.
30. Do M. Melanopsin and the Intrinsically Photosensitive Retinal Ganglion Cells: Biophysics to Behavior. NEURON. [Journal Article; Research Support, N.I.H., Extramural; Research Support, Non-U.S. Gov't; Review]. 2019 2019-10-23;104(2):205 – 26.
31. Tomita Y, Qiu C, Bull E, Allen W, Kotoda Y, Talukdar S, et al. Muller glial responses compensate for degenerating photoreceptors in retinitis pigmentosa. EXP MOL MED. [Journal Article; Research Support, N.I.H., Extramural; Research Support, Non-U.S. Gov't]. 2021 2021-11-01;53(11):1748–58.
32. Goel M, Dhingra NK. Muller glia express rhodopsin in a mouse model of inherited retinal degeneration. NEUROSCIENCE. [Journal Article; Research Support, Non-U.S. Gov't]. 2012 2012-12-06;225:152 – 61.
33. Hanzelmann S, Castelo R, Guinney J. GSVA: gene set variation analysis for microarray and RNA-seq data. BMC BIOINFORMATICS. [Journal Article; Research Support, N.I.H., Extramural; Research Support, Non-U.S. Gov't]. 2013 2013-01-16;14:7.

34. Ghai K, Zelinka C, Fischer AJ. Notch signaling influences neuroprotective and proliferative properties of mature Muller glia. J NEUROSCI. [Journal Article; Research Support, N.I.H., Extramural]. 2010 2010-02-24;30(8):3101–12.
35. Liu B, Hunter DJ, Rooker S, Chan A, Paulus YM, Leucht P, et al. Wnt signaling promotes Muller cell proliferation and survival after injury. Invest Ophthalmol Vis Sci. [Comparative Study; Journal Article; Research Support, Non-U.S. Gov't]. 2013 2013-01-17;54(1):444–53.
36. Guttenplan KA, Stafford BK, El-Danaf RN, Adler DI, Munch AE, Weigel MK, et al. Neurotoxic Reactive Astrocytes Drive Neuronal Death after Retinal Injury. CELL REP. [Journal Article; Research Support, N.I.H., Extramural; Research Support, Non-U.S. Gov't]. 2020 2020-06-23;31(12):107776.
37. Aibar S, Gonzalez-Blas CB, Moerman T, Huynh-Thu VA, Imrichova H, Hulselmans G, et al. SCENIC: single-cell regulatory network inference and clustering. NAT METHODS. [Journal Article]. 2017 2017-11-01;14(11):1083–6.
38. Butler A, Hoffman P, Smibert P, Papalexi E, Satija R. Integrating single-cell transcriptomic data across different conditions, technologies, and species. NAT BIOTECHNOL. [Journal Article; Research Support, N.I.H., Extramural; Research Support, U.S. Gov't, Non-P.H.S.]. 2018 2018-06-01;36(5):411–20.
39. Haque M, Siegel RJ, Fox DA, Ahmed S. Interferon-stimulated GTPases in autoimmune and inflammatory diseases: promising role for the guanylate-binding protein (GBP) family. Rheumatology (Oxford). [Journal Article; Research Support, N.I.H., Extramural; Research Support, Non-U.S. Gov't; Review]. 2021 2021-02-01;60(2):494–506.
40. Rivett AJ, Bose S, Brooks P, Broadfoot KI. Regulation of proteasome complexes by gamma-interferon and phosphorylation. BIOCHIMIE. [Journal Article; Research Support, Non-U.S. Gov't; Review]. 2001 2001-03-01;83(3–4):363–6.
41. Lahne M, Nagashima M, Hyde DR, Hitchcock PF. Reprogramming Muller Glia to Regenerate Retinal Neurons. ANNU REV VIS SCI. [Journal Article; Research Support, N.I.H., Extramural; Research Support, Non-U.S. Gov't; Review]. 2020 2020-09-15;6:171 – 93.
42. Hayflick SJ. Defective pantothenate metabolism and neurodegeneration. Biochem Soc Trans. [Journal Article; Research Support, N.I.H., Extramural; Research Support, Non-U.S. Gov't; Review]. 2014 2014-08-01;42(4):1063-8.
43. Li W, Tanikawa T, Kryczek I, Xia H, Li G, Wu K, et al. Aerobic Glycolysis Controls Myeloid-Derived Suppressor Cells and Tumor Immunity via a Specific CEBPB Isoform in Triple-Negative Breast Cancer. CELL METAB. [Journal Article]. 2018 2018-07-03;28(1):87–103.
44. Rauen T, Benedyk K, Juang YT, Kerkhoff C, Kyttaris VC, Roth J, et al. A novel intronic cAMP response element modulator (CREM) promoter is regulated by activator protein-1 (AP-1) and accounts for altered activation-induced CREM expression in T cells from patients with systemic lupus erythematosus. J BIOL CHEM. [Journal Article; Research Support, Non-U.S. Gov't]. 2011 2011-09-16;286(37):32366–72.
45. Hirai S, Miwa A, Ohtaka-Maruyama C, Kasai M, Okabe S, Hata Y, et al. RP58 controls neuron and astrocyte differentiation by downregulating the expression of Id1-4 genes in the developing cortex.

EMBO J. [Journal Article; Research Support, Non-U.S. Gov't]. 2012 2012-03-07;31(5):1190–202.

46. Simo R, Stitt AW, Gardner TW. Neurodegeneration in diabetic retinopathy: does it really matter? DIABETOLOGIA. [Journal Article; Research Support, N.I.H., Extramural; Research Support, Non-U.S. Gov't; Review]. 2018 2018-09-01;61(9):1902–12.
47. Kim SA, Kim SJ, Choi YA, Yoon HJ, Kim A, Lee J. Retinal VEGFA maintains the ultrastructure and function of choriocapillaris by preserving the endothelial PLVAP. Biochem Biophys Res Commun. [Journal Article; Research Support, Non-U.S. Gov't]. 2020 2020-01-29;522(1):240–6.
48. Lyu Z, Jin H, Yan Z, Hu K, Jiang H, Peng H, et al. Effects of NRP1 on angiogenesis and vascular maturity in endothelial cells are dependent on the expression of SEMA4D. INT J MOL MED. [Journal Article]. 2020 2020-10-01;46(4):1321–34.
49. Shih YP, Yuan SY, Lo SH. Down-regulation of DLC1 in endothelial cells compromises the angiogenesis process. CANCER LETT. [Journal Article; Research Support, N.I.H., Extramural]. 2017 2017-07-10;398:46–51.
50. Jensen LD, Hot B, Ramskold D, Germano R, Yokota C, Giatrellis S, et al. Disruption of the Extracellular Matrix Progressively Impairs Central Nervous System Vascular Maturation Downstream of beta-Catenin Signaling. Arterioscler Thromb Vasc Biol. [Journal Article; Research Support, N.I.H., Extramural; Research Support, Non-U.S. Gov't]. 2019 2019-07-01;39(7):1432–47.
51. Veys K, Fan Z, Ghobrial M, Bouche A, Garcia-Caballero M, Vriens K, et al. Role of the GLUT1 Glucose Transporter in Postnatal CNS Angiogenesis and Blood-Brain Barrier Integrity. CIRC RES. [Journal Article; Research Support, Non-U.S. Gov't]. 2020 2020-07-31;127(4):466–82.
52. Prete M, Dammacco R, Fatone MC, Racanelli V. Autoimmune uveitis: clinical, pathogenetic, and therapeutic features. CLIN EXP MED. [Journal Article; Review]. 2016 2016-05-01;16(2):125–36.
53. Caspi R. Autoimmunity in the immune privileged eye: pathogenic and regulatory T cells. IMMUNOL RES. [Journal Article; Review]. 2008 2008-01-20;42(1–3):41–50.
54. Zhong Z, Su G, Kijlstra A, Yang P. Activation of the interleukin-23/interleukin-17 signalling pathway in autoinflammatory and autoimmune uveitis. PROG RETIN EYE RES. [Journal Article; Research Support, Non-U.S. Gov't; Review]. 2021 2021-01-01;80:100866.
55. Hysa E, Cutolo CA, Gotelli E, Pacini G, Schenone C, Kreps EO, et al. Immunopathophysiology and clinical impact of uveitis in inflammatory rheumatic diseases: An update. EUR J CLIN INVEST. [Journal Article; Review]. 2021 2021-08-01;51(8):e13572.
56. Broderick CA, Smith AJ, Balaggan KS, Georgiadis A, Buch PK, Trittibach PC, et al. Local administration of an adeno-associated viral vector expressing IL-10 reduces monocyte infiltration and subsequent photoreceptor damage during experimental autoimmune uveitis. MOL THER. [Letter; Research Support, Non-U.S. Gov't]. 2005 2005-08-01;12(2):369–73.
57. Lee YS, Amadi-Obi A, Yu CR, Egwuagu CE. Retinal cells suppress intraocular inflammation (uveitis) through production of interleukin-27 and interleukin-10. IMMUNOLOGY. [Journal Article; Research Support, N.I.H., Intramural]. 2011 2011-04-01;132(4):492–502.

58. Ng SS, De Labastida RF, Yan J, Corvino D, Das I, Zhang P, et al. The NK cell granule protein NKG7 regulates cytotoxic granule exocytosis and inflammation. NAT IMMUNOL. [Journal Article; Research Support, N.I.H., Extramural; Research Support, Non-U.S. Gov't]. 2020 2020-10-01;21(10):1205–18.
59. Ruvolo PP, Ruvolo VR, Benton CB, AlRawi A, Burks JK, Schober W, et al. Combination of galectin inhibitor GCS-100 and BH3 mimetics eliminates both p53 wild type and p53 null AML cells. Biochim Biophys Acta. [Journal Article; Research Support, N.I.H., Extramural]. 2016 2016-04-01;1863(4):562–71.
60. Wildner G, Diedrichs-Mohring M. Resolution of uveitis. SEMIN IMMUNOPATHOL. [Journal Article; Review]. 2019 2019-11-01;41(6):727–36.
61. Kanehisa M, Sato Y, Kawashima M, Furumichi M, Tanabe M. KEGG as a reference resource for gene and protein annotation. NUCLEIC ACIDS RES. [Journal Article; Research Support, Non-U.S. Gov't]. 2016 2016-01-04;44(D1):D457-62.
62. Lin W, Zhou S, Feng M, Yu Y, Su Q, Li X. Soluble CD83 Regulates Dendritic Cell-T Cell Immunological Synapse Formation by Disrupting Rab1a-Mediated F-Actin Rearrangement. Front Cell Dev Biol. [Journal Article]. 2020 2020-01-20;8:605713.
63. Heuss ND, Lehmann U, Norbury CC, McPherson SW, Gregerson DS. Local activation of dendritic cells alters the pathogenesis of autoimmune disease in the retina. J IMMUNOL. [Journal Article; Research Support, N.I.H., Extramural; Research Support, Non-U.S. Gov't]. 2012 2012-02-01;188(3):1191–200.
64. Wang P, Sun SH, Silver PB, Chan CC, Agarwal RK, Wiggert B, et al. Methimazole protects from experimental autoimmune uveitis (EAU) by inhibiting antigen presenting cell function and reducing antigen priming. J Leukoc Biol. [Journal Article; Research Support, Non-U.S. Gov't]. 2003 2003-01-01;73(1):57–64.
65. Jamali A, Kenyon B, Ortiz G, Abou-Slaybi A, Sendra VG, Harris DL, et al. Plasmacytoid dendritic cells in the eye. PROG RETIN EYE RES. [Journal Article; Research Support, N.I.H., Extramural; Research Support, Non-U.S. Gov't; Review]. 2021 2021-01-01;80:100877.
66. Lin W, Liu T, Wang B, Bi H. The role of ocular dendritic cells in uveitis. IMMUNOL LETT. [Journal Article; Research Support, Non-U.S. Gov't; Review]. 2019 2019-05-01;209:4–10.
67. Cao EY, Ouyang JF, Rackham O. GeneSwitches: ordering gene expression and functional events in single-cell experiments. BIOINFORMATICS. [Journal Article; Research Support, Non-U.S. Gov't]. 2020 2020-05-01;36(10):3273–5.
68. Ippolito GC, Dekker JD, Wang YH, Lee BK, Shaffer AR, Lin J, et al. Dendritic cell fate is determined by BCL11A. Proc Natl Acad Sci U S A. [Journal Article; Research Support, N.I.H., Extramural; Research Support, N.I.H., Intramural; Research Support, Non-U.S. Gov't]. 2014 2014-03-18;111(11):E998-1006.
69. Gamboa-Cedeno AM, Castillo M, Xiao W, Waldmann TA, Ranuncolo SM. Alternative and canonical NF-kB pathways DNA-binding hierarchies networks define Hodgkin lymphoma and Non-Hodgkin diffuse large B Cell lymphoma respectively. J Cancer Res Clin Oncol. [Journal Article]. 2019 2019-06-01;145(6):1437–48.

70. Yu C, Roubeix C, Sennlaub F, Saban DR. Microglia versus Monocytes: Distinct Roles in Degenerative Diseases of the Retina. TRENDS NEUROSCI. [Journal Article; Research Support, N.I.H., Extramural; Research Support, Non-U.S. Gov't; Review]. 2020 2020-06-01;43(6):433–49.
71. Veinotte L, Gebremeskel S, Johnston B. CXCL16-positive dendritic cells enhance invariant natural killer T cell-dependent IFNgamma production and tumor control. ONCOIMMUNOLOGY. [Journal Article; Research Support, Non-U.S. Gov't]. 2016 2016-06-01;5(6):e1160979.
72. Crish SD, Dapper JD, MacNamee SE, Balaram P, Sidorova TN, Lambert WS, et al. Failure of axonal transport induces a spatially coincident increase in astrocyte BDNF prior to synapse loss in a central target. NEUROSCIENCE. [Journal Article; Research Support, N.I.H., Extramural; Research Support, Non-U.S. Gov't]. 2013 2013-01-15;229:55–70.
73. Insua MF, Simon MV, Garelli A, de Los SB, Rotstein NP, Politi LE. Trophic factors and neuronal interactions regulate the cell cycle and Pax6 expression in Muller stem cells. J NEUROSCI RES. [Journal Article; Research Support, Non-U.S. Gov't]. 2008 2008-05-15;86(7):1459–71.
74. Goldman D. Muller glial cell reprogramming and retina regeneration. NAT REV NEUROSCI. [Journal Article; Research Support, N.I.H., Extramural; Research Support, Non-U.S. Gov't; Review]. 2014 2014-07-01;15(7):431 – 42.
75. Yu G, Wang LG, Han Y, He QY. clusterProfiler: an R package for comparing biological themes among gene clusters. OMICS. [Journal Article; Research Support, Non-U.S. Gov't]. 2012 2012-05-01;16(5):284–7.
76. Gene Ontology Consortium: going forward. NUCLEIC ACIDS RES. [Journal Article; Research Support, N.I.H., Extramural]. 2015 2015-01-01;43(Database issue):D1049-56.
77. Liberzon A, Birger C, Thorvaldsdottir H, Ghandi M, Mesirov JP, Tamayo P. The Molecular Signatures Database (MSigDB) hallmark gene set collection. CELL SYST. [Journal Article]. 2015 2015-12-23;1(6):417–25.
78. Ritchie ME, Phipson B, Wu D, Hu Y, Law CW, Shi W, et al. limma powers differential expression analyses for RNA-sequencing and microarray studies. NUCLEIC ACIDS RES. [Journal Article; Research Support, Non-U.S. Gov't]. 2015 2015-04-20;43(7):e47.
79. Qiu X, Mao Q, Tang Y, Wang L, Chawla R, Pliner HA, et al. Reversed graph embedding resolves complex single-cell trajectories. NAT METHODS. [Journal Article]. 2017 2017-10-01;14(10):979–82.

Figures

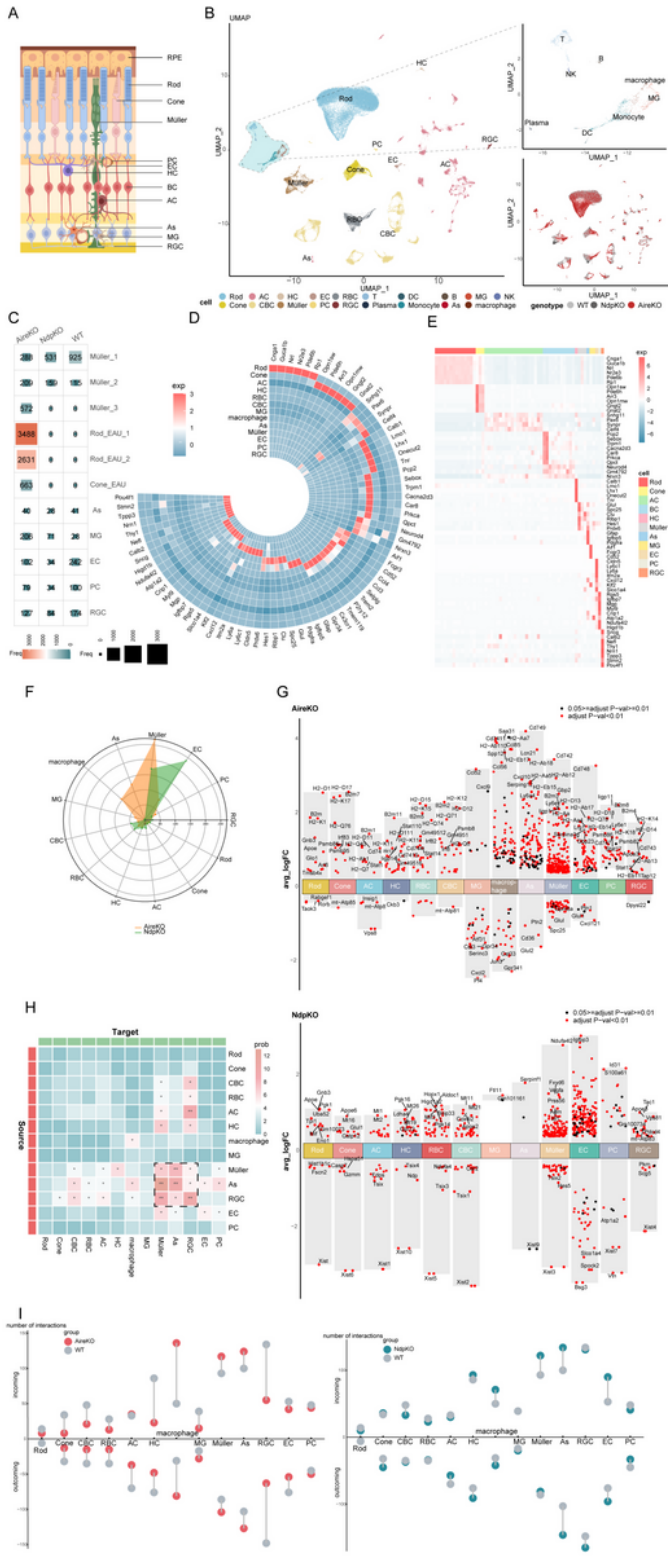

Figure 1

A single-cell atlas of the mouse retina in the normal state and two pathological states. (A) Schematic diagram of the retina. In addition to photoreceptor cells, rods and cones, there are glial cells (Müller cells, microglia, astrocytes), bipolar cells (BCs), horizontal cells (HCs), amacrine cells (ACs), vascular endothelial cells, pericytes and retinal ganglion cells (RGCs). The neurovascular unit (NVU) is composed of neuron-glia-vessels, including RGCs, astrocytes, microglia, vascular endothelial cells, perivascular cells,

basement membranes and extracellular matrix. (B) All cell types in the integrated dataset, cells unique to AireKO data and three different samples are shown separately in UMAP plots. (C) The numbers of different samples for specific cells. Large numbers are in red, and small numbers are in blue. The size of the rectangle also represents the number. (D) Circular heatmap showing the markers for each cell type. High expression is in red, and low expression is in blue. (E) The marker in Figure 1(D) was used to validate the P14 dataset, and the heatmap shows the expression of the marker. High expression is in red, and low expression is in blue. (F) Radar plot showing the number of DEGs in different cell types in AireKO and NdpKO samples compared to WT samples. (G) DEGs in different cell types in AireKO and NdpKO samples compared to WT samples. The colors of the dots represent different P-values. (H) The heatmap shows the communication relationships between cells. The source is the sender of the signal, the target is the receiver, and more asterisks indicate stronger communication. Strong communication is shown in red, and weak communication is shown in blue. (I) Numbers of interactions for each cell as sender and receiver in AireKO and NdpKO samples compared to WT samples.

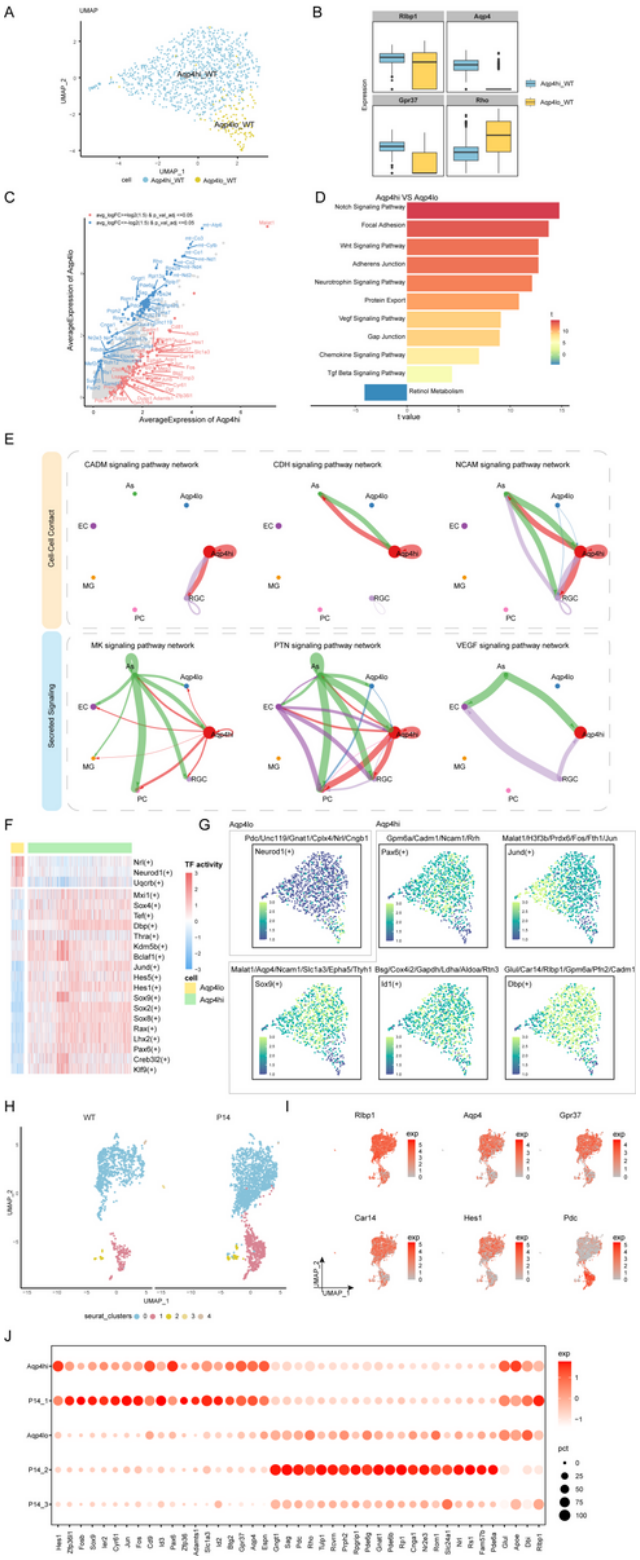

Figure 2

Exploration and validation of two subpopulations of Müller cells. (A) UMAP plot showing two subclusters of Müller cells in WT mice. (B) The boxplot shows the marker genes of two subclusters of Müller cells. (C) Volcano plot showing differences in gene expression between Aqp4^{hi} and Aqp4^{lo} cells. Genes with |avg_logFC| ≥ 1 and adjusted p value < 0.01 are labeled. (D) Bar graphs show GSVA pathway analysis for Aqp4^{hi} and Aqp4^{lo} cells, with colors representing t values. (E) Significant signaling networks. Circle sizes

are proportional to the number of cells in each cell group, and edge width represents the communication probability. (F) Heatmap showing the activity of important TFs in Aqp4^{hi} cells and Aqp4^{lo} cells according to AUCell. (G) UMAP showing the expression of specific TF target genes. The color from dark to light represents increased expression. (H) The UMAP plot shows that there are two subclusters of cells highly similar to Aqp4^{hi} and Aqp4^{lo} cells in the P14 data. (I) Featureplot shows the expression of marker genes in the integrated data. (J) The bubble plot shows new markers for the different cells we identified. The color of the target gene represents the expression, and the size of the circle represents the percentage.

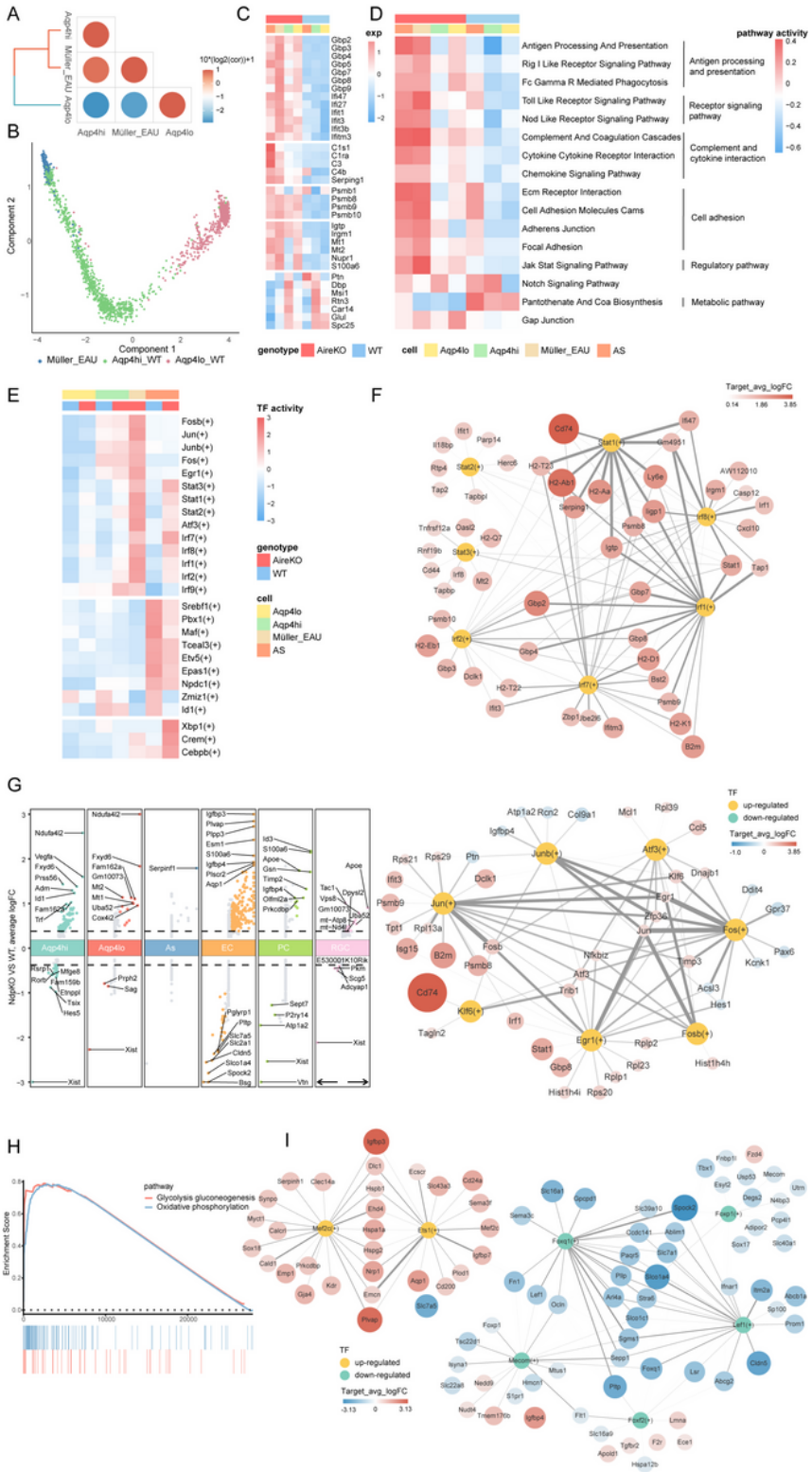

Figure 3

Phenotypic changes and underlying mechanisms of the NVU in two models. (A) Bubble plot and dendrogram show correlations among the three Müller cell groups. The value represented by the color is calculated by 10*(log10(cor))+1. (B) Cell trajectory of Aqp4^{hi}, Aqp4^{lo} and Müller_EAU. (C) The heatmap shows the important cytokines of Müller cells and As in AireKO and WT mice. High expression is in red, and low expression is in blue. (D) The heatmap shows the pathways of Müller cells and As in AireKO and

WT mice. Pathways are divided into different categories. (E) Heatmap shows the activity of important TFs of different cell types according to AUCell. (F) The network diagram shows the important TFs in Müller_EAU and their downstream target gene associations. TFs that were upregulated are shown in yellow, while those that were downregulated are shown in green, and the color of the target gene represents the avg_logFC; the size of the circle represents the abs(avg_logFC), and the line thickness represents importance. We selected the top 20 genes by Target_avg_exp * importance value among the target genes with importance >5 for each TF. (G) Volcano plot showing the differences in the gene expression of $Aqp4^{hi}$, $Aqp4^{lo}$, As, EC, PC and RGC populations in NdpKO compared to WT mice. Genes with |avg_logFC| > log2(1.3) and adjusted p value< 0.01 are labeled. (H) GSEA revealed that $Aqp4^{hi}$ cells in NdpKO mice showed upregulation of metabolism-related pathways. (I) The network diagram shows the important TFs in ECs and their downstream target gene associations. TFs that were upregulated are shown in yellow, while those that were downregulated are shown in green, and the color of the target gene represents the avg_logFC; the size of the circle represents the abs(avg_logFC), and the line thickness represents importance. We selected the top 20 genes by the Target_avg_exp*importance value among the target genes with importance > 5 for each TF.

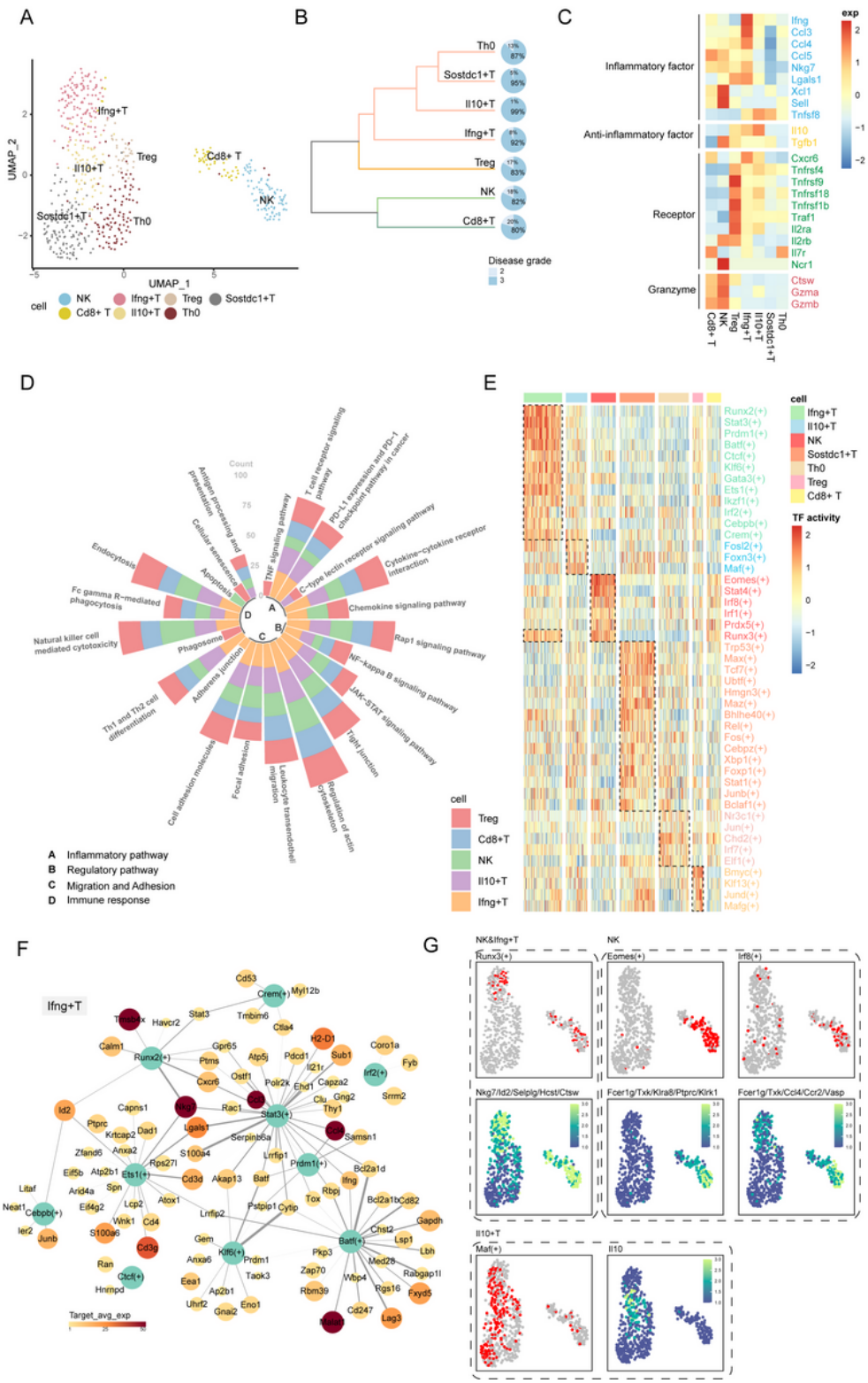

Figure 4

(A) UMAP plot shows the subclusters of T and NK cells. (B) The dendrogram shows the relationships between subclusters of T and NK cells, with different colors representing different species. Pie charts show the proportion of cell numbers for different grades of disease for each cell type. (C) Heatmap showing important cytokines in T and NK cells, and the cytokines are divided into different categories. High expression is in red, and low expression is in blue. (D) Circular bar graph shows KEGG pathway

enrichment results in different cells; these pathways are grouped into different categories. The length of the bar graph represents the sum of the counts in each cell for each pathway. (E) Heatmap showing important transcription factors for different cell types in the SCENIC analysis results. (F) The network diagram shows the important TFs in *Ifng*$^{+}$T cells and their downstream target gene associations. All TFs are in green, and the color of the target gene represents the expression; the size of the circle represents the pct, and the line thickness represents importance. We selected the top 25 genes by Target_avg_exp * importance value among the target genes with importance > 5 for each TF. (G) UMAP plots show important TFs and their target genes for NK, NK and *Ifng*$^{+}$ T, and *Il10*$^{+}$ T cells.

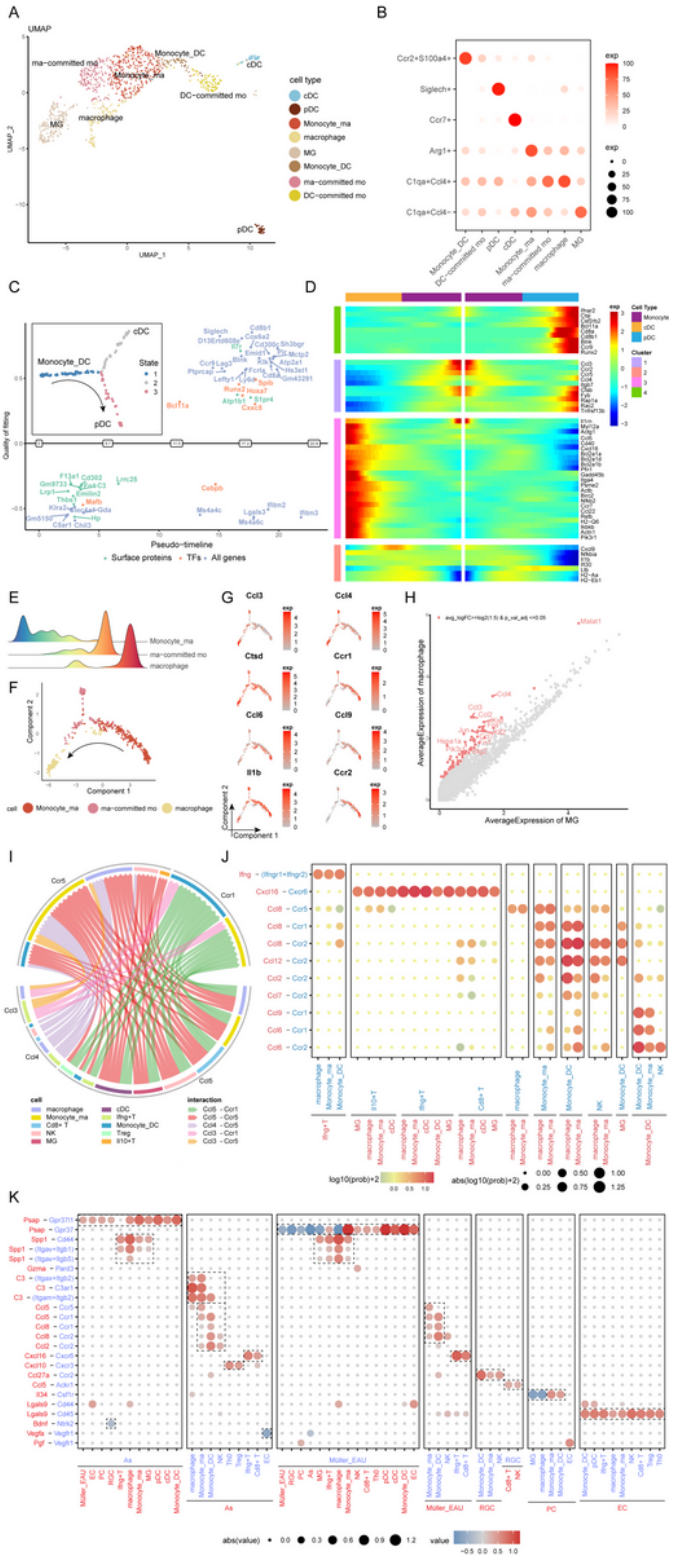

Figure 5

Immune regulatory network, monocytes and their derived cells in AireKO mice. (A) UMAP plot shows cells in the MG lineage, Ma-monocyte lineage and DC-monocyte lineage. (B) The bubble chart shows the marker genes of different cells, and the color and size represent the proportion of cells expressing the gene in a cell type. (C) UMAP shows the trajectory from state 1 to state 3. Significant surface proteins, transcription factors (TFs), and all genes are also shown along pseudotime. (D) Heatmap shows branch

expression analysis modeling of monocytes between cDCs (left) and pDCs (right). (E) Ridge plot shows the distribution of the Ma monocyte lineage along pseudotime. (F) Cell trajectory of the Ma monocyte lineage. (G) Featureplot shows the expression of important cytokines along the cell trajectory. (H) Volcano plot showing differences in gene expression between macrophages and MGs in AireKO mice. Genes with |avg_logFC| ≥ 1 and adjusted p value <= 0.01 are labeled. (I) The chord diagram shows the communication links between cells, and different cells and interactions are represented by different colors. (J) Comparison of the significant ligand–receptor pairs. The color and the point size indicate the value of log10 (communication probability) + 2. Ligands and signal senders are marked in red, while receptors and receivers of signals are marked in blue. (K) Comparison of the significant ligand–receptor pairs between NdpKO and WT mice. We define the value as log10 (difference in communication probability) + 2, and the color and the point size indicate the value. Ligands and signal senders are marked in red, while receptors and receivers of signals are marked in blue. Important ligand receptor pairs are presented in boxes.

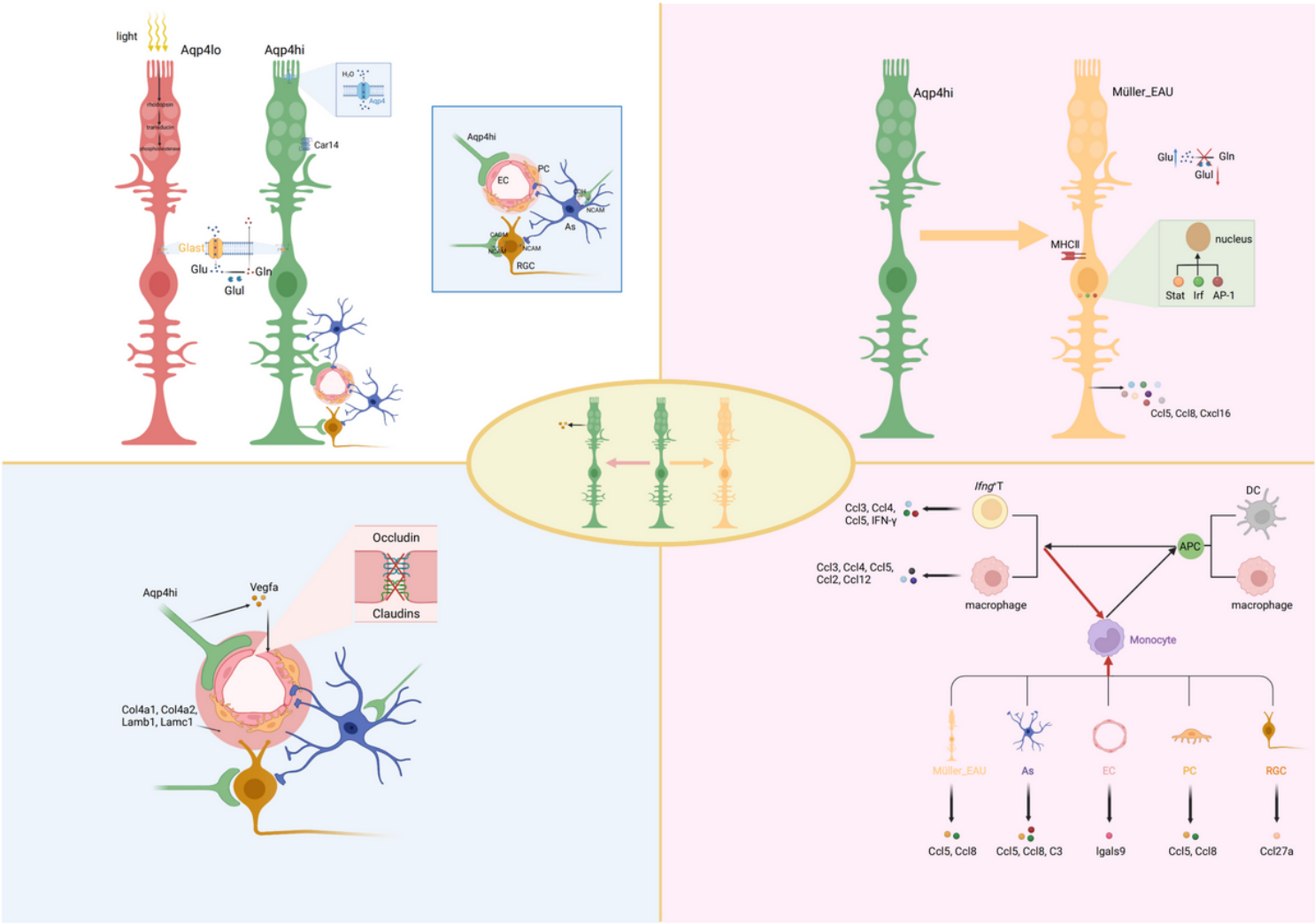

Figure 6

Overview of the key findings of our study. Different subclusters of Müller cells exist, and Aqp4^{hi} cells are degenerated in AireKO mice. Differential changes in the NVU structure in EAU and FEVR compared to WT

conditions and closed-loop regulation of NVU cells and inflammatory cells in EAU were identified. This image was created with BioRender.com.

Supplementary Files

This is a list of supplementary files associated with this preprint. Click to download.

- SupplementaryMaterial.docx